

**ELECTROCHEMICAL INVESTIGATION OF DOPAMINE
NEUROTRANSMISSION INVOLVING IONTOPHORESIS**

by
Andrew Seipel

A dissertation submitted to the faculty of the University of North Carolina at Chapel Hill in
partial fulfillment of the requirements for the degree of Doctor of Philosophy in the
Department of Chemistry

Chapel Hill
2007

Approved by

Advisor: R. Mark Wightman

Readers: Mark Schoenfisch

James Jorgenson

Paul Manis

Robert Rosenberg

ABSTRACT

**ANDREW SEIPEL: Electrochemical investigation of dopamine neurotransmission involving iontophoresis
(Under the direction of Dr. R. Mark Wightman)**

Identification of the role of transient dopamine release in behavior has proved difficult. In order to interpret the complex processes involved in dopamine neurotransmission, dopamine release and cell firing rates must be recorded and the signals correlated through pharmacological manipulation. For this purpose, the carbon-fiber electrodes employed for electrochemical dopamine detection and extracellular unit recordings were combined with the local drug delivery technique, iontophoresis.

The application of glutamate, dopamine, and the glutamate receptor antagonist, CNQX, by iontophoresis strongly modulated cell firing rates in anesthetized rats with short (20 s) ejections. The ejection of glutamate and the dopamine receptor agonist, quinpirole HCl, strongly decreased stimulated dopamine release though required ejections several minutes long. The stimulated dopamine release studies are believed to require greater distances the ejected compound must diffuse in order to generate a detectable effect. This increased distance may explain the drastic difference in ejection durations. Glutamate was found to increase firing in a minority of neurons and no observed effect from dopamine in freely-moving animals. However, long ejections of the D1 antagonist, SCH23390, inhibited cell firing during ICSS behavior.

The amount of basal dopamine present in the extracellular fluid was also studied. Dopamine levels were monitored during microinjection of saline and lidocaine in the ventral tegmental area and systemic cocaine administration. With both impulse-dependent dopamine release and dopamine reverse transport blocked, minimal decreases in dopamine were observed (< 25 nM) that are similar to levels obtained in recent microdialysis estimates.

A novel action of cocaine was also investigated using genetically-modified mice. The effect of cocaine upon stimulated dopamine release in mice lacking all 3 isoforms of the protein, synapsin, was investigated using fast-scan cyclic voltammetry and amperometry. Cocaine was found to increase dopamine release through not only decreasing uptake but through increasing the amount of dopamine released per stimulus event. During depleting (15 second) electrical stimulations and after synthesis inhibition via α -methyl-para-tyrosine administration, the synapsin TKO mice showed a decreased response to cocaine with respect to wild-type mice. This suggests an interaction between a synapsin-dependent pool of dopamine vesicles and cocaine.

ACKNOWLEDGEMENTS

There are several people to whom I am indebted to whose efforts and instruction were integral in completing this work. I would especially like to thank Dr. Mark Wightman for his continual leadership and support throughout my graduate career.

I would also like to acknowledge the aid of Dr. George Rebec, Dr. Leslie Sombers, Dr. Joseph Cheer, Dr. Michael Johnson, Natalie Rios-Herr, and Manna Beyene with the slice and behavior experiments and Jill Venton with the synapsin experiments.

TABLE OF CONTENTS

	Page
LIST OF FIGURES	ix
LIST OF ABBREVIATIONS AND SYMBOLS	xi
 Chapter	
I. Investigating dopamine neurotransmission	1
Introduction.....	2
Traditional tools to study the postsynaptic actions of neurotransmitters.....	3
Recording methods	4
Preparations.....	5
Methods to introduce pharmacological probes	6
Dopamine receptors	10
Pre-synaptic effects.....	11
Post-synaptic effects	13
Other neurotransmitters	15
Conclusion	16
References.....	17
II. Experimental techniques	21
Introduction.....	22
Electrochemistry	22
Instrumentation	22

Fast scan cyclic voltammetry	23
Amperometry	26
Data analysis	28
Kinetic parameters	28
Principle component regression.....	29
Electrophysiology	29
Injections.....	31
Iontophoresis.....	31
References.....	39
III. Iontophoresis in anesthetized rats	41
Introduction.....	42
Methods.....	44
Results.....	47
Glutamate and dopamine effects on single unit activity.....	47
Glutamate effects on stimulated dopamine release.....	47
Effect of dopaminergic agents on dopamine release	48
Systemic application of raclopride.....	53
Discussion	53
Conclusion	59
References.....	61
IV. Iontophoresis in freely-moving rats.....	64
Introduction.....	65
Methods.....	66

Results.....	68
Discussion.....	69
Conclusion	75
References.....	76
V. Estimating the basal dopamine level with fast scan cyclic voltammetry.....	78
Introduction.....	79
Methods.....	80
Results.....	81
Discussion.....	86
Blocking sources of extracellular dopamine.....	86
Previous basal level estimates.....	88
Using rapid concentration changes to estimate basal levels	90
Conclusion	91
References.....	93
VI. Cocaine Increases Dopamine Release by Mobilization of a Synapsin-Dependent Reserve Pool	96
Introduction.....	97
Methods.....	98
Surgery	98
Electrochemistry	99
Data analysis	99
Drugs.....	100
Results.....	100

Effects of cocaine on electrically evoked dopamine release	100
Effects of cocaine on dopamine release after synthesis inhibition	101
Discussion	105
Cocaine increases dopamine release probability	105
Synapsins regulate releasable stores in dopamine neurons.....	106
Implications of synapsin regulation of dopamine release.....	107
References	109

LIST OF FIGURES

Figure 2.1	Image of carbon-fiber microelectrode	23
Figure 2.2	Diagram of color plot formulation	27
Figure 2.3	Image of 4-barrel iontophoresis probe	33
Figure 2.4	Ejection characteristics of iontophoresis probes	34
Figure 2.5	Localization of iontophoresis ejection in vitro	37
Figure 2.6	Localization of iontophoresis ejection in vivo	38
Figure 3.1	The effect of quinpirole iontophoresis upon stimulated dopamine release ...	49
Figure 3.2	The effect of raclopride administration upon stimulated dopamine release..	50
Figure 3.3	The effect of raclopride on quinpirole inhibition	51
Figure 3.4	The effect of glutamate iontophoresis upon stimulated dopamine release....	52
Figure 3.5	Effect of dopamine iontophoresis upon glutamate-excited cell activity	54
Figure 3.6	The effect of glutamate iontophoresis upon cell activity	55
Figure 4.1	D1 dependence of tonic firing	70
Figure 4.2	D1 affect on patterned firing	71
Figure 4.3	Effect of glutamate iontophoresis on spontaneously-active neurons	72
Figure 4.4	Effect of dopamine iontophoresis on spontaneously-active neurons.....	73
Figure 5.1	Saline microinjection.....	83
Figure 5.2	Lidocaine microinjection.....	84
Figure 5.3	Average dopamine response to saline and lidocaine microinjection.....	85
Figure 5.4	Cocaine and lidocaine injection.....	87
Figure 6.1	Effects of cocaine on dopamine release evoked by 900 pulse, 60 Hz electrical stimulations	101

Figure 6.2	Effects of α -MPT followed by cocaine administration on stimulated dopamine release in WT and synapsin TKO mice	99..... 103
------------	--	-------------

LIST OF ABBREVIATIONS AND SYMBOLS

AMPA	α -amino-3-hydroxy-methylisoxazole-4-propionic acid hydrate
cAMP	cyclic adenosine monophosphate
CNQX	6-cyano-7-nitroquinoxaline -2,3-dione
DA	dopamine
[DA] _p	dopamine released per pulse
DARPP	dopamine-regulated phosphoprotein
DAT	dopamine transporter
EPSC	excitatory post-synaptic current
EPSP	excitatory post-synaptic potential
FSCV	fast scan cyclic voltammetry
GPCR	G-protein-coupled receptor
HEPES	N-[2-hydroxyethyl]piperazine-N-[2-ethanesulfonic acid] buffer
ICSS	intercranial self-stimulation
K _m	affinity of dopamine for DAT
KO	knock out
MFB	medial forebrain bundle
mGluR	metabotropic glutamate receptor
MSN	medium spiny neuron
NAc	nucleus accumbens
NMDA	n-methyl-d-aspartate
PCR	principle component regression
PKAc	catalytic subunit of protein kinase A

SEM	scanning electron microscopy
TH	tyrosine hydroxylase
TKO	triple knock out
Tris	tris(hydroxymethyl)aminomethane buffer
UEI	universal electrochemical instrument
VGlut	vesicular glutamate transporter
VMAT	vesicular monoamine transporter
V_{\max}	maximum rate of dopamine uptake
VTA	ventral tegmental area

CHAPTER 1:
INVESTIGATING DOPAMINE NEUROTRANSMISSION

INTRODUCTION

With the development of techniques capable of measuring neurotransmitter concentrations within the living brain, the characteristics of the spontaneous release of dopamine are being revealed. An overall view of the relevant biochemical pathways is of critical importance to understand the ways in which the chemical signals can affect neural signaling pathways.

The class of neurotransmitter receptors known as ionotropic receptors produces immediate effects upon ion conductance and membrane potentials because they are directly linked to ion channels. Like most neurons, mammalian medium spiny neurons (MSNs), the target of dopaminergic neurons, have a resting potential of around -85 mV. Increasing the conductance of sodium channels through activation of ionotropic receptors will shift the membrane potential to more positive values and thus may trigger an action potential. By opening potassium channels through interactions with specific receptors, neurotransmitters can hyperpolarize the cell thereby reducing the probability of action potential generation. Opening calcium channels will modulate neurotransmitter release as well as impact protein phosphorylation within the cell. By measuring the conductance of these specific receptor-linked channels and their effects on membrane potentials, electrophysiologists can record and unravel the effects of neurotransmitters that interact with ionotropic receptors.

In contrast, all identified dopamine receptors belong the class of receptors known as G-protein coupled receptors (GPCR). Unlike ionotropic receptors, the GPCRs are not

directly linked to ion channels [1]. Rather GPCRs modulate neuronal activity through interactions with a G-protein complex [2]. When activated by the binding of a neurotransmitter, the α subunit dissociates from the γ , β complex and the receptor. The α subunit then interacts with other proteins within the neuron, triggering a signaling cascade capable of producing a variety of effects from modulating ion channel conductance to regulating protein expression. Activation of GPCRs can produce effects that last only milliseconds to changes that persist for hours or longer. Through combination of electrophysiology and molecular biology experiments, the complex effect of dopamine receptor activation is being characterized.

Advances over the last few decades in analytical sampling techniques have allowed dopamine to be measured during behavior. The next step is to define its role by correlating presynaptic dopamine signals with changes in the firing rate of post-synaptic neurons. The initial stage is investigation of the properties of dopamine receptors and factors involved in modulating its release. In order to reach the final goal, both a means of producing a dopamine signal or measuring a spontaneous release event as well as a method to observe changes in firing rate at the same location are required. In addition, the role of dopamine in changes in firing rate must be confirmed through introduction of pharmacological compounds to the system.

TRADITIONAL TOOLS TO STUDY THE POSTSYNAPTIC ACTIONS OF NEUROTRANSMITTERS

To study the effects of dopamine release, methods are required to both introduce dopamine to neurons as well as detect changes in neuronal activity. The systems in

which dopamine effects have been studied vary greatly in complexity, and range from single cultured neurons to neurons in awake and behaving animals. The choice of biological preparation determines what dopamine sources and detection methods are optimal.

Recording methods

Electrophysiological methods sample the electrical properties of neurons and provide the most rapid, direct measurement of the effect of a neurotransmitter upon a neuron. Intracellular methods require inserting an electrode into a cell. The electrode can be used in current clamp mode in which voltage changes, termed excitatory post-synaptic potential (EPSP), are monitored when ion channels open in response to receptor activation. Alternatively the electrode can be used in voltage clamp mode in which current changes, termed excitatory post-synaptic current (EPSC) are monitored. Patch clamp involves attaching a capillary to the membrane to form a high resistance seal at which current and voltage clamp experiments are performed. Patch clamp is capable of measuring the activity of a subset of ion channels on a cell membrane. Such intracellular techniques are commonly used with cell culture or slice experiments where the neurons are readily accessible by the experimenter. For in vivo preparations, extracellular recordings are frequently performed where changes in potential caused by ion flow from an action potential are measured at a distance from the target neuron.

Preparations

Cultured neurons allow the environment to be precisely controlled and facilitate intracellular recording techniques. Neurons isolated in cultures undergo adaptive changes and often form synapses with themselves, known as autapses, instead of synapses. Co-culture with glia and other neurons may improve the similarity to in vivo preparations. Another approach is to use brain slices. In this preparation the results are affected by the thickness and direction in which they are sliced. Coronal slices are produced by taking a thin slice laterally from the top to the bottom of the brain. Coronal slices do not contain whole dopamine neurons, but only the dopamine terminals and their targets, the cell bodies of medium spiny neurons. Nevertheless, the terminals still release dopamine. Sagittal and horizontal slices can contain whole dopamine neurons along with medium spiny neurons. Sagittal slices are vertical slices along the entire length of the brain. Horizontal slices encompass the entire length of the brain along the horizontal plane. All slice preparations differ from in vivo preparations due to a lack of neurotransmitter tone and incomplete neural circuits [3].

For measurements in the intact brain, both anesthetized and freely moving animals have been investigated. Chloral hydrate and urethane are commonly used as anesthetics and chemical or electrical sensors are entered into the brain regions of interest through small holes in the skull. During experiments under anesthesia, the animal is usually placed in a stereotaxic apparatus which holds the animal in place and allows the use of micromanipulators for precise positioning of electrodes. Anesthesia causes drastic changes in neural activity however [4]. Although technically more difficult to perform, experiments in freely moving animals provide the most physiologically-relevant data

since the neurons have experienced the least changes from normal conditions. Dopamine effects in these experiments occur with proper tonic neurotransmitter levels and neural activity. Moreover, freely moving experiments are the only method in which dopamine changes can be directly correlated to behavior.

Methods to introduce pharmacological probes

A variety of sources have been developed which allow introduction of either dopamine or selective agonists and antagonists. The major techniques are systemic administration, microinjection, reverse dialysis, iontophoresis and chemical or electrical stimulation.

In systemic application, the compound is introduced to the entire preparation, either through injection into the blood stream for animal preparations or introduction to the bath solution for cell and slice preparations. Though relatively simple, systemic techniques have several limitations, particularly in intact brain preparations. Many compounds can not be administered in this manner due to their inability to cross the blood/brain barrier and the entire brain is affected by the injection, convoluting results with changes up or downstream in the neural circuitry originating in other brain regions. Systemic applications are slow in comparison to transient dopamine signals, often requiring several minutes for onset to occur and complete clearance may take hours or even days.

Microinjection is the injection of small volumes of a drug solution directly into the desired brain region. Able to target a subsection of the brain and circumvent the blood/brain barrier, microinjection offers many advantages over systemic application. A

related technique is reverse dialysis with a microdialysis probe. A compound capable of crossing the dialysis membrane is added to the buffer and diffuses from the probe into the sampling region. Both techniques greatly improve the spatial resolution for drug application, but are still relatively slow and capable of mimicking slow, tonic dopamine level changes in a given region but not rapid dopamine signaling.

Iontophoresis is used to generate transient changes in dopamine concentrations. Iontophoresis applies large, local concentrations of a compound with a net ionic charge which are ejected within a few seconds using an applied current. While producing large concentrations, iontophoresis only ejects small quantities of ions therefore clearance by diffusion is rapid. The amount of a given compound ejected follows the equation:

$$M = n \frac{iT}{ZF}$$

The amount ejected in moles, M , is proportional to the ratio of the ejection current (i) and ejection time (T) to the charge (Z) and Faraday's constant (F) [5]. This ratio is modified by n , the ejection efficiency coefficient, which is empirically derived and varies significantly between electrodes thereby making the technique only quantitative if direct measurement of ejection from each iontophoresis barrel is obtained [6]. For this reason, iontophoresis in most applications is not quantitative.

Iontophoresis suffers from several other disadvantages. When the ejected compound is not directly monitored, discriminating between an unresponsive cell and unsuccessful ejection is difficult [7]. At large ejection currents iontophoresis may even

influence the activity of a neuron independent of the compound actually being ejected and discriminating between excitation and disinhibition is not possible [1]. Pairing iontophoresis with a detection technique allows for concentrations and confirmation of ejection to be obtained, circumventing some of the key disadvantages of the technique.

Endogenous dopamine release can be evoked by chemical or electrical stimulation of dopamine neurons. The stimulation can be performed either at the terminals, or for preparations with complete neurons, at the cell bodies. Used with coronal brain slices, local electrical stimulation evokes release that is of similar duration to spontaneous dopamine transients. However, it may generate electrical interference with electrochemical or electrophysiological measurements. Because nerve terminals from non-dopaminergic cells are interspersed with dopamine nerve terminals, local stimulation will also generate release of other neurotransmitters in addition to dopamine. Chemical stimulation often employs potassium or n-methyl-d-aspartate (NMDA). Potassium application depolarizes the cell, forcing voltage-dependent ion channels to open and generate an action potential. The application of NMDA activates excitatory ionotropic glutamate receptors known as NMDA receptors which depolarize the cell and generate an action potential. Chemical stimulation and trains of electrical pulses at the cell bodies are referred to as remote stimulations. Remote stimulation is the most common stimulation method for in vivo preparations and can produce short duration dopamine release events similar to physiological release events. Because the stimulation occurs far from the terminal region, only neurons that project from the stimulated region to the terminal field will release neurotransmitter within the region. This gives remote methods greater selectivity, although co-stimulation of other neurons may still occur. Also of importance

to interpretation of data from stimulated release experiments is that the release generated is synchronous. All neurons within the stimulated region release neurotransmitter simultaneously with remote and local stimulations, which may not be an appropriate model for physiological release events.

One example of the non-selective nature of stimulation occurred in a study of electrically stimulated dopamine release [8]. Dopamine release was generated via electrical stimulation in the MFB and both dopamine release and changes in post-synaptic cell firing were simultaneously measured. Inhibition and excitation in response to the stimulation were recorded that coincided with the lifetime of dopamine release. For the cells inhibited by the stimulation, systemic injection of the vesicular monoamine transporter blocker, Ro4-1284, abolished dopamine release but not the inhibition. Systemic bicuculline administration, a GABA_A antagonist, abolished the inhibition which led to the conclusion that the inhibition was caused by stimulating GABAergic neurons in the MFB and dopamine release did not primarily impact neuronal activity. These findings reveal a deficiency in the selectivity electrical and chemical stimulation of dopamine cell bodies which can obscure dopamine actions.

The selection of recording technique, animal model, and drug delivery technique controls what information regarding dopamine neurotransmission can be obtained. Each technique and model will introduce their own set of experimental confounds that must be considered in interpretation of the results. Through analysis of the unique observations obtained from the various recording techniques and animal models, a view of dopamine neurotransmission can be formed.

DOPAMINE RECEPTORS

Several dopamine receptors have been identified. The receptors currently known have been placed into two primary groups based upon pharmacological specificity: the D1 family, which includes D₁ and D₅ receptors, and the D2 family, populated by D₂, D₃, and D₄ receptors. The D₁, D₂, and D₃ receptors show high expression levels in the NAc [9]. All known dopamine receptors are G-protein coupled receptors (GPCR) which are not directly linked to ion channels [1].

Dopamine receptors have been found to interact with potassium, sodium, and calcium channels through adenylate cyclase that converts ATP into the second messenger, cAMP [10]. Investigations of the specific signaling cascades involving D1 and D2 receptors found that a key molecular target for post-synaptic dopamine receptor activation is the protein DARPP-32. The DARPP-32 protein contains multiple phosphorylation sites. Depending upon the sites phosphorylated, DARPP-32 is capable of interacting with various protein phosphatases involved in cascades required for signal amplification and integration [11]. Recent models employing current knowledge of signaling cascades from D1 receptor activation showed that modulation of cAMP-dependent kinase (PKAc) and DARPP-32 persists for several hundred milliseconds longer than the duration of the receptor activation [12]. Genetically-modified DARPP-32 knockout (KO) mice that lack the DARPP-32 protein have been produced. The DARPP-32 KO mice display a decreased ability of dopamine to modulate ion channels and long-term neuronal activity. The KO mice have even displayed attenuated responses to several drugs of abuse such as increased movement after cocaine or amphetamine administration [13].

Because GPCR effects are indirect, they occur on a slower timescale than ionotropic receptor effects [14]. This delay is compounded by the design of dopaminergic synapses in which dopamine transporters and receptors are located outside of the synapse [15]. The net result is that dopamine must diffuse a greater distance to reach its receptors in comparison to synaptic neurotransmitters such as glutamate. The extra-synaptic action of dopamine has led to the label “volume” transmitter and dopamine release events are believed to affect multiple targets [16, 17]. The delay for onset of dopamine-receptor mediated signals raises the question as to whether dopamine influences a response to the stimulus event that generated the signal [14]. A key example of dopamine’s delay was shown with observation of two distinct responses to dopamine neuron stimulation [18]. A short, rapid-onset excitation was followed by a second delayed excitation lasting several seconds after electrical stimulation of the MFB. The initial excitation was due to co-stimulation of glutamate neurons and not dopaminergic in nature, while the delayed onset signal was found to be due to dopamine release. The experiments estimated that dopamine receptor effects upon neuronal activity have a delay of at least 200 ms from the release event till effects are witnessed.

Pre-synaptic effects

Dopamine receptors are located on the pre-synaptic terminals of dopamine neurons. Through these receptors, dopamine can inhibit subsequent release events. Auto-inhibition of dopamine release is primarily a D2 mediated effect. When dopamine is released, pre-synaptic D2 receptors are activated and trigger a cascade that leads to a

decrease in calcium channel conductance and downregulation of tyrosine hydroxylase (TH), an enzyme necessary for dopamine synthesis [19-22].

Experiments characterizing autoreceptor function were performed in rat brain slices and anesthetized rats using amperometry to detect dopamine release from a pair of electrical stimulus trains with differing temporal separations between each stimulation [3, 23]. Comparison of the relative maximum release from each stimulation allowed characterization of the timescale of D2 receptor effects. The data showed the modulation of dopamine release with sub-second resolution and obtained an overall time window of 200 ms to 5 s with maximal inhibition at 700ms in slices. A maximal inhibition between 150-300 ms after the stimulation with the effect disappearing within 600 ms was observed in the anesthetized experiment.

The role of D2 autoreceptors in dopamine signaling is more complex than simple inhibition of release. A recent study used pharmacology to probe the role of D2 receptors on stimulated dopamine release measured by FSCV in the rat brain [24]. Depression or potentiation is defined as decreased or increased dopamine release when compared to the initial pulse train, respectively. Neurons were found to show depression of dopamine release with the application of raclopride, a D2 antagonist. Quinpirole, a D2 agonist, generated a potentiation of dopamine release from the pulse trains. Though the exact mechanism is unknown, the findings indicate that D2 autoreceptor activation can lead to desensitization of their effects during exposure to large amounts of dopamine.

Other neurotransmitters may modulate release from dopaminergic nerve terminals as well. Experiments in cultured neurons, slices, and anesthetized animals have shown that dopamine release is strongly inhibited by increased glutamate levels [25-27]. Some

controversy exists over the receptor responsible for the inhibition, with both mGluR5 and a signaling cascade initiated by AMPA receptors activation [28, 29]. The AMPA receptor cascade involves production of hydrogen peroxide which then modulates potassium channel conductance, decreasing dopamine release [29]. The mechanism involved in the mGluR5 has not been explored currently. Nevertheless, the experiments are all evidence for the influence of tonic glutamate levels upon dopamine release.

Post-synaptic effects

Dopaminergic neurons project onto medium spiny neurons throughout the striatum. These neurons also receive glutamatergic input as well originating from the hippocampus, amygdala, pre-frontal cortex, and thalamus [15, 30]. The current hypothesis for the role of dopamine is that it gates the incoming glutamatergic signals [31]. Dopamine is postulated to act as a filter and increases the “signal to noise” of a given target neuron’s activity [32]. As discussed previously, the extrasynaptic receptors suggest dopamine acts across numerous dendrites and pre-synaptic terminals. Dopamine release would saturate the region surrounding the release site with relatively slow onset and offset and modulate the neuron’s response to glutamatergic inputs.

Intracellular electrophysiological recordings in anesthetized rats have shown the existence of up and down states in medium spiny neurons [33]. Medium spiny neurons are dormant in the down state (approximately -85 mV). The MSN partially depolarizes to approximately -55 mV when entering the up state. Once in the upstate, the neuron more readily generates action potentials in response to glutamatergic inputs. The driving force behind neurons entering the up state appears to be glutamate [34]. Dopamine

interacts with the states with opposing effects from D1 and D2 receptors [35]. The activation of D1 receptors increases the conductance of L-type calcium channels and NMDA receptors, stabilizing the neuron in the upstate [36-38]. Stabilization of the up state leads to enhanced excitability of the MSN. Alternatively, activation of D2 receptors reduces the conductance of calcium channels and excitatory AMPA receptors thereby reducing MSN excitability by destabilizing the up state [37, 39]. However, recent experiments using intracellular recordings in unanesthetized rats found that MSNs displayed only a single state in awake animals [40]. When asleep, the neurons displayed the predicted two-state behavior observed in anesthetized, slice and cell preparations. This result calls into question the up and down-state hypothesis to interpret recordings from behaving animals.

Extracellular recordings, which are unable to distinguish up and down states, from anesthetized and freely moving animals have shown primarily inhibition in response to dopamine for spontaneously active and glutamate-excited cells [10]. Dopamine and amphetamine ejection via iontophoresis produced inhibition that was blocked by both D1 and D2 antagonists [41]. Stimulation of dopamine neurons has also produced excitatory effects from dopamine release. NMDA injection into the medial forebrain bundle produced an excitation that lasted for 1 s after the stimulation were observed, The excitation was sensitive to D1 receptor activation and antagonism [42].

Experiments by Millar and Williams used voltammetric recordings to correlate dopamine quantities produced by various electrical stimulus trains with changes in MSN cell activity [43]. Medium spiny neurons displayed excitations in response to sub-micromolar dopamine release and inhibitions from release events producing more than 1

μ M dopamine. Both responses to dopamine were abolished by administration of alpha-methyl-para-tyrosine (AMPT) which blocks dopamine synthesis and thus abolishes vesicular dopamine release. The experiment was later successfully replicated using introduction of dopamine via iontophoresis [44]. Both D1 and D2 receptors were found to be involved in the excitations.

These experiments, while providing supporting evidence to the actions of dopamine, fall short of a complete view of dopamine neurotransmission. To understand the actions of dopamine in complex behaviors, the spontaneous release of dopamine need to be measured in real-time and correlated to cell firing in freely-moving animals.

Other neurotransmitters

Evidence is emerging that suggests dopamine terminals may release glutamate in addition to dopamine. Currently, the expression of one type of vesicular glutamate transporter, the VGlut2, has been shown in neurons that stain positive for tyrosine hydroxylase (TH) [45, 46]. The transporter is only expressed in a subset of DA neurons, and the majority of synapses formed by these neurons do not display morphology typical of glutamatergic synapses [47]. Strong expression of VGlut3 has been observed in the striatum and accumbens [4]. The co-expression of VGlut3 and serotonin, acetylcholine, and GABA neurons has been observed in other brain regions, though not in TH-positive neurons at this time [48, 49].

Indirect electrophysiological evidence exists in cultured neurons and slices that support co-release of glutamate. Investigation of dopamine neuron autapses, which are formed when a neuron forms a synapse with itself, observed EPSPs that are blocked by

NMDA receptor antagonists in addition to dopamine receptor antagonists [50]. Brain slices can also display both a rapid and long-delay onset EPSC in response to stimulation, with the rapid onset signal sensitive only to glutamate receptor antagonist, CNQX [51]. Correcting for potential confounds such as co-release of other neurotransmitters requires full pharmacological analysis of post-synaptic effects.

CONCLUSION

Investigating the role of dopamine in neural activity is a complex task. Improvement of detection techniques makes real-time measurement of dopamine release possible. In order to form a complete view of dopamine neurotransmission, the interaction between factors modulating release, post-synaptic firing rates, and intracellular signaling need to be investigated. A wealth of information regarding the actions of dopamine in cultured cells, brain slices, and anesthetized animals has been produced to date. The next step in advancing the field is correlating in real-time the pre-synaptic dopamine release events with post-synaptic cell firing in awake, behaving animals. In such a complex system, the potential for non-dopaminergic effects convoluting the interpretation of results is high. The next development is pairing the recording techniques with local drug delivery systems such as iontophoresis to confirm dopamine's actions.

REFERENCES

1. Neve, K. and R. Neve, *The Dopamine Receptors*. The Receptors. 1997.
2. Greengard, P., *The neurobiology of slow synaptic transmission*. Science, 2001. **294**(5544): p. 1024-30.
3. Phillips, P.E., P.J. Hancock, and J.A. Stamford, *Time window of autoreceptor-mediated inhibition of limbic and striatal dopamine release*. Synapse, 2002. **44**(1): p. 15-22.
4. Warenycia, M.W. and G.M. McKenzie, *Responses of striatal neurons to anesthetics and analgesics in freely moving rats*. Gen Pharmacol, 1984. **15**(6): p. 517-22.
5. Hicks, T.P., *The history and development of microiontophoresis in experimental neurobiology*. Prog Neurobiol, 1984. **22**(3): p. 185-240.
6. Armstrong-James, M., et al., *Quantitative iontophoresis of catecholamines using multibarrel carbon fibre microelectrodes*. J Neurosci Methods, 1981. **4**(4): p. 385-406.
7. Bloom, F.E., *To spritz or not to spritz: the doubtful value of aimless iontophoresis*. Life Sci, 1974. **14**(10): p. 1819-34.
8. Cheer, J.F., et al., *Simultaneous dopamine and single-unit recordings reveal accumbens GABAergic responses: implications for intracranial self-stimulation*. Proc Natl Acad Sci U S A, 2005. **102**(52): p. 19150-5.
9. Sealfon, S.C. and C.W. Olanow, *Dopamine receptors: from structure to behavior*. Trends Neurosci, 2000. **23**(10 Suppl): p. S34-40.
10. Nicola, S.M., J. Surmeier, and R.C. Malenka, *Dopaminergic modulation of neuronal excitability in the striatum and nucleus accumbens*. Annu Rev Neurosci, 2000. **23**: p. 185-215.
11. Svenningsson, P., et al., *DARPP-32: an integrator of neurotransmission*. Annu Rev Pharmacol Toxicol, 2004. **44**: p. 269-96.
12. Lindskog, M., et al., *Transient calcium and dopamine increase PKA activity and DARPP-32 phosphorylation*. PLoS Comput Biol, 2006. **2**(9): p. e119.
13. Fienberg, A.A., et al., *DARPP-32: regulator of the efficacy of dopaminergic neurotransmission*. Science, 1998. **281**(5378): p. 838-42.

14. Di Chiara, G., et al., *Dopamine and drug addiction: the nucleus accumbens shell connection*. Neuropharmacology, 2004. **47 Suppl 1**: p. 227-41.
15. Sesack, S.R., et al., *Anatomical substrates for glutamate-dopamine interactions: evidence for specificity of connections and extrasynaptic actions*. Ann N Y Acad Sci, 2003. **1003**: p. 36-52.
16. Venton, B.J., et al., *Real-time decoding of dopamine concentration changes in the caudate-putamen during tonic and phasic firing*. J Neurochem, 2003. **87**(5): p. 1284-95.
17. Garris, P.A., et al., *Efflux of dopamine from the synaptic cleft in the nucleus accumbens of the rat brain*. J Neurosci, 1994. **14**(10): p. 6084-93.
18. Gonon, F., *Prolonged and extrasynaptic excitatory action of dopamine mediated by D1 receptors in the rat striatum in vivo*. J Neurosci, 1997. **17**(15): p. 5972-8.
19. Cardozo, D.L. and B.P. Bean, *Voltage-dependent calcium channels in rat midbrain dopamine neurons: modulation by dopamine and GABAB receptors*. J Neurophysiol, 1995. **74**(3): p. 1137-48.
20. O'Hara, C.M., et al., *Inhibition of dopamine synthesis by dopamine D2 and D3 but not D4 receptors*. J Pharmacol Exp Ther, 1996. **277**(1): p. 186-92.
21. Onali, P. and M.C. Olanas, *Involvement of adenylate cyclase inhibition in dopamine autoreceptor regulation of tyrosine hydroxylase in rat nucleus accumbens*. Neurosci Lett, 1989. **102**(1): p. 91-6.
22. Lindgren, N., et al., *Dopamine D(2) receptors regulate tyrosine hydroxylase activity and phosphorylation at Ser40 in rat striatum*. Eur J Neurosci, 2001. **13**(4): p. 773-80.
23. Benoit-Marand, M., E. Borrelli, and F. Gonon, *Inhibition of dopamine release via presynaptic D2 receptors: Time course and functional characteristics in vivo*. Journal of Neuroscience, 2001. **21**(23): p. 9134-9141.
24. Kita, J.M., et al., *Paradoxical modulation of short-term facilitation of dopamine release by dopamine D2 receptors*. Journal of Neuroscience
25. Wu, Y., et al., *Inhibitory glutamatergic regulation of evoked dopamine release in striatum*. Neuroscience, 2000. **96**(1): p. 65-72.
26. Avshalumov, M.V., et al., *Glutamate-dependent inhibition of dopamine release in striatum is mediated by a new diffusible messenger, H2O2*. J Neurosci, 2003. **23**(7): p. 2744-50.

27. Kulagina, N.V., M.J. Zigmond, and A.C. Michael, *Glutamate regulates the spontaneous and evoked release of dopamine in the rat striatum*. Neuroscience, 2001. **102**(1): p. 121-8.
28. Zhang, H. and D. Sulzer, *Glutamate spillover in the striatum depresses dopaminergic transmission by activating group I metabotropic glutamate receptors*. J Neurosci, 2003. **23**(33): p. 10585-92.
29. Avshalumov, M.V., et al., *Endogenous hydrogen peroxide regulates the excitability of midbrain dopamine neurons via ATP-sensitive potassium channels*. J Neurosci, 2005. **25**(17): p. 4222-31.
30. Grace, A.A., et al., *Regulation of firing of dopaminergic neurons and control of goal-directed behaviors*. Trends Neurosci, 2007.
31. West, A.R., et al., *Electrophysiological interactions between striatal glutamatergic and dopaminergic systems*. Ann N Y Acad Sci, 2003. **1003**: p. 53-74.
32. Kiyatkin, E.A. and G.V. Rebec, *Dopaminergic modulation of glutamate-induced excitations of neurons in the neostriatum and nucleus accumbens of awake, unrestrained rats*. J Neurophysiol, 1996. **75**(1): p. 142-53.
33. Wickens, J.R. and C.J. Wilson, *Regulation of action-potential firing in spiny neurons of the rat neostriatum in vivo*. J Neurophysiol, 1998. **79**(5): p. 2358-64.
34. Goto, Y. and P. O'Donnell, *Network synchrony in the nucleus accumbens in vivo*. J Neurosci, 2001. **21**(12): p. 4498-504.
35. West, A.R. and A.A. Grace, *Opposite influences of endogenous dopamine D1 and D2 receptor activation on activity states and electrophysiological properties of striatal neurons: studies combining in vivo intracellular recordings and reverse microdialysis*. J Neurosci, 2002. **22**(1): p. 294-304.
36. Levine, M.S., et al., *Modulatory actions of dopamine on NMDA receptor-mediated responses are reduced in D1A-deficient mutant mice*. J Neurosci, 1996. **16**(18): p. 5870-82.
37. Cepeda, C., N.A. Buchwald, and M.S. Levine, *Neuromodulatory actions of dopamine in the neostriatum are dependent upon the excitatory amino acid receptor subtypes activated*. Proc Natl Acad Sci U S A, 1993. **90**(20): p. 9576-80.
38. Surmeier, D.J., et al., *Modulation of calcium currents by a D1 dopaminergic protein kinase/phosphatase cascade in rat neostriatal neurons*. Neuron, 1995. **14**(2): p. 385-97.

39. Hernandez-Lopez, S., et al., *D2 dopamine receptors in striatal medium spiny neurons reduce L-type Ca²⁺ currents and excitability via a novel PLC[β 1-IP3-calcineurin-signaling cascade*. J Neurosci, 2000. **20**(24): p. 8987-95.
40. Mahon, S., et al., *Distinct patterns of striatal medium spiny neuron activity during the natural sleep-wake cycle*. J Neurosci, 2006. **26**(48): p. 12587-95.
41. Kiyatkin, E.A. and G.V. Rebec, *Iontophoresis of amphetamine in the neostriatum and nucleus accumbens of awake, unrestrained rats*. Brain Res, 1997. **771**(1): p. 14-24.
42. Gonon, F. and L. Sundstrom, *Excitatory effects of dopamine released by impulse flow in the rat nucleus accumbens in vivo*. Neuroscience, 1996. **75**(1): p. 13-8.
43. Williams, G.V. and J. Millar, *Concentration-dependent actions of stimulated dopamine release on neuronal activity in rat striatum*. Neuroscience, 1990. **39**(1): p. 1-16.
44. Hu, X.T. and F.J. White, *Dopamine enhances glutamate-induced excitation of rat striatal neurons by cooperative activation of D1 and D2 class receptors*. Neurosci Lett, 1997. **224**(1): p. 61-5.
45. Trudeau, L.E., *Glutamate co-transmission as an emerging concept in monoamine neuron function*. Journal of Psychiatry & Neuroscience, 2004. **29**(4): p. 296-310.
46. Kawano, M., et al., *Particular subpopulations of midbrain and hypothalamic dopamine neurons express vesicular glutamate transporter 2 in the rat brain*. Journal of Comparative Neurology, 2006. **498**(5): p. 581-592.
47. Lapish, C.C., J.K. Seamans, and L. Judson Chandler, *Glutamate-dopamine cotransmission and reward processing in addiction*. Alcohol Clin Exp Res, 2006. **30**(9): p. 1451-65.
48. Fremeau, R.T., et al., *The identification of vesicular glutamate transporter 3 suggests novel modes of signaling by glutamate*. Proceedings of the National Academy of Sciences of the United States of America, 2002. **99**(22): p. 14488-14493.
49. Herzog, E., et al., *Localization of VGLUT3, the vesicular glutamate transporter type 3, in the rat brain*. Neuroscience, 2004. **123**(4): p. 983-1002.
50. Sulzer, D., et al., *Dopamine neurons make glutamatergic synapses in vitro*. J Neurosci, 1998. **18**(12): p. 4588-602.
51. Chuhma, N., et al., *Dopamine neurons mediate a fast excitatory signal via their glutamatergic synapses*. J Neurosci, 2004. **24**(4): p. 972-81.

CHAPTER 2

EXPERIMENTAL TECHNIQUES

INTRODUCTION

The detection of neurotransmitter release and cell action potentials requires the use of several specialized measurement and data analysis techniques. In this section, the methods used for detecting and analyzing dopamine release, cell unit activity, and drug delivery are discussed in detail. The data obtained using these methods are discussed in subsequent chapters.

ELECTROCHEMISTRY

Instrumentation

The electrodes employed for in vivo analysis of dopamine release were carbon-fiber microelectrodes. The small dimensions of the probe ($\sim 5\text{-}7\text{ }\mu\text{m}$ diameter) cause minimal damage to tissue in the sampled region and have spatial resolution dependent upon electrode length [1]. The electrodes were fabricated using T650 carbon fibers pulled in a glass capillary tube using a vertical pipette puller (Narishige International USA, East Meadow, NY) and cut to a 50 to 100 μm length. An SEM image of a single-barrel carbon-fiber electrode is shown in **Figure 2.1**. Electrical contact between the carbon fiber and lead wire was achieved with a high conductivity solution (9 M sodium acetate, 250 mM potassium chloride) or conductive silver paint. The electrodes were attached via a headstage to either an EI-400 (Ensmann Instrumentation, Bloomington, IN) for in vitro measurements or a UEI potentiostat (UNC Electronics Facility, Chapel Hill, NC) for in vivo experiments. The

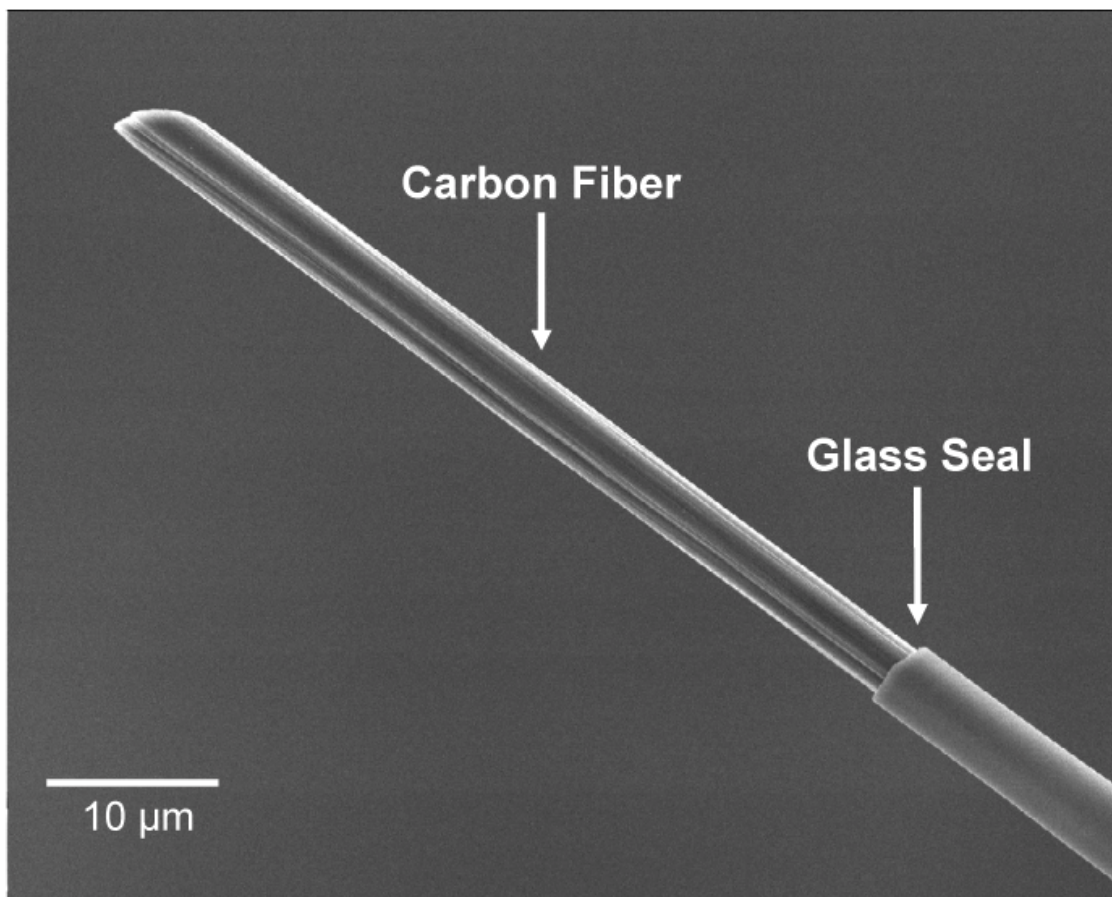


Figure 2.1: Image of carbon-fiber microelectrode. A SEM of a carbon-fiber microelectrode made with a T-650 carbon fiber in a single microcapillary tube.

interface between the potentiostat and the computer was the UEI breakout panel.

Silver/silver chloride reference electrodes were fabricated by application of a low voltage to a silver wire in 0.1 M HCl for several seconds until a uniform white coating covered the surface.

Fast scan cyclic voltammetry

Dopamine was measured using fast scan cyclic voltammetry (FSCV) and constant potential amperometry. For catecholamines, the electrode is held at a negative potential between applications of a triangle waveform, which ramps to a positive potential above the oxidation potential and then returns to the holding potential at hundreds of volts per second. During the oxidative scan, dopamine at the surface of the electrode is oxidized to dopamine-*o*-quinone. Any quinone at the surface of the electrode during the reductive scan is reduced back to dopamine. Carbon is a desirable material for this technique due to its highly adsorptive properties. During the application of the holding potential, cations can adsorb to the electrode surface. The strength of adsorption leads to a proportionate increase in sensitivity to the species [2]. During the ramp application, a large charging current is generated due to rapid flow of ions in the double layer. The charging current is orders of magnitude greater than the faradaic currents produced by physiologically-relevant concentrations of dopamine. For a 50 μm long carbon fiber electrode, background currents are approximately 300 to 900 nA depending upon the scan rate employed. The faradaic current generated at 0.6 V from the oxidation of 250 nM dopamine is only a few nanoamps or less. To remove the charging current and also faradaic current from interfering compounds such as ascorbic acid, cyclic

voltammograms (CV) are produced by subtracting CVs containing changes in dopamine concentration from background CVs lacking detectable dopamine changes. Significant drift in the charging current is detected with FSCV over long time periods. The exact causes for the charging current drift are unknown, but it is minimized by limiting background subtractions to less than 90 seconds.

The exact voltage at which the electrode is held at between waveform applications and the oxidative voltage the ramp reaches significantly effects the results. Increasing the scan limits to higher oxidative currents appears to modify the surface characteristics of the carbon fibers, leading to stronger adsorption but a decrease in selectivity [3]. The increase in adsorption further decreases the time response and clouds information about uptake kinetics. Increasing scan limits also increases the charging current, often requiring the use of a low gain headstage or reduced electrode length. The waveform used is therefore tailored to the specific experiment with respect to what information is desired and sensitivity requirements.

Two ramps were used throughout the experiments. The first, commonly called the traditional waveform, has the electrode held at -0.4 V, increased to 1.0 V, and then lowered back to -0.4 V at 300 V/s. The second waveform, known as the intermediate waveform, has increased scan limits from -0.4 V to 1.3 V at a scan rate of 400 V/s. Both waveforms are applied at 10 Hz for data collection. All electrodes were cycled at 60 Hz for 10 minutes before beginning the experiment in order to obtain a stable response. Waveform characteristics were input and data collected using a Labview-based program. Calibration of electrodes for FSCV was performed by flowing plugs of known dopamine concentrations past the electrode using a 6-port LC valve driven by a pneumatic actuator.

Calibrations for the traditional waveform used HEPES buffer, while the intermediate waveform required use of TRIS buffer. Both buffers were adjusted to physiological pH.

The frequent collection of cyclic voltammograms generates large amounts of information throughout the course of an experiment. With 150 voltammograms generated over the course of the usual 15 second file a method in which both the quantitative and qualitative information could be rapidly conveyed was necessary. In order to achieve this, cyclic voltammograms are plotted in graphs, referred to as color plots. The color plots are generated by graphing the voltammograms sequentially along the x-axis and voltage displayed along the y-axis. The current generated at the electrode for a given voltage is displayed in false color. A diagram of the formulation of color plots is shown in **Figure 2.2**.

Amperometry

Constant potential amperometry's primary advantage is superior temporal resolution and sensitivity compared to FSCV [4]. The technique is also useful for experiments investigating kinetic parameters involved with dopamine release events such as rates of uptake and neurotransmitter release per pulse due to a lack of adsorption which distorts observed kinetic data [5]. For dopamine measurements, amperometry consists of holding the electrode at 0.3V for the duration of data collection.

Amperometry data was collected at 60 Hz and passed through an external low-pass filter (Krohn-Hite, Brockton, MA) set to 30 Hz. Due to insufficient chemical selectivity, dopamine release in a given site was confirmed with FSCV prior to amperometric analysis. All data was collected using a Labview-based amperometry program.

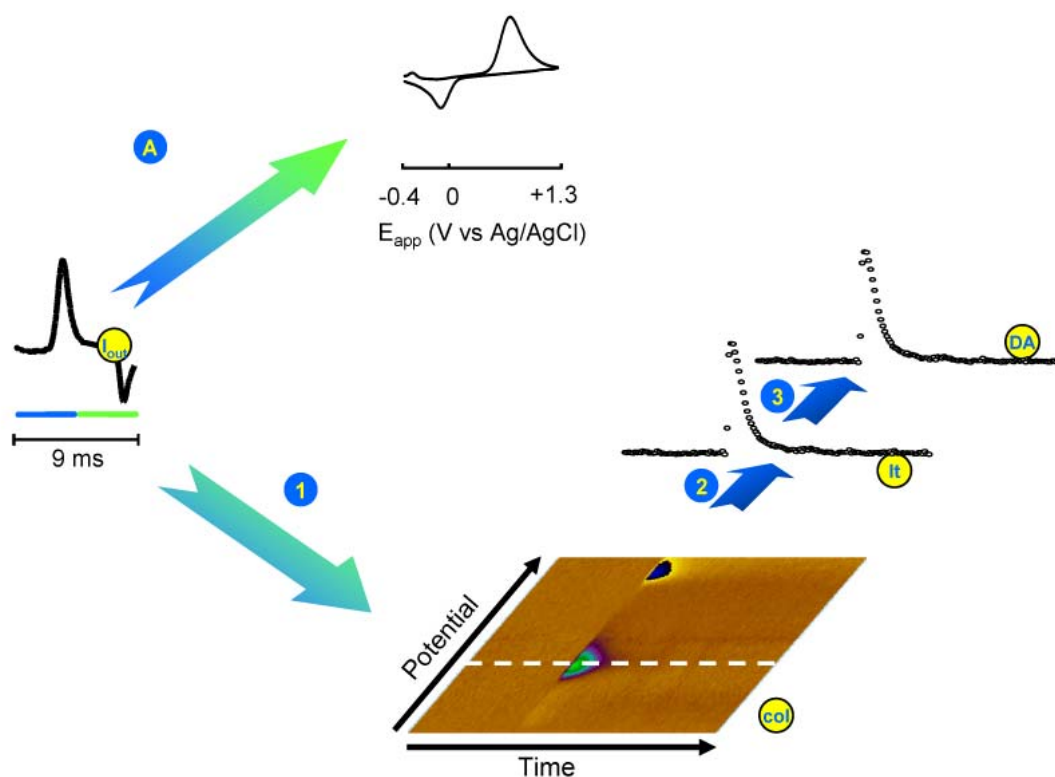


Figure 2.2: Diagram of color plot formulation. A) Cyclic voltammograms are plotted versus potential to provide chemical verification. 1.) Successive voltammograms are plotted with time along the x-axis, potential along the y-axis, and current displayed in false color. 2.) A potential at which the analyte is oxidized or reduced is selected and the current at that potential across all voltammograms is used to produce the current versus time trace. 3.) Through in vitro calibration, the current trace is converted to a concentration versus time trace.

DATA ANALYSIS

Kinetic parameters

The detection of dopamine in the extrasynaptic space provides the opportunity to measure key factors in dopamine neurotransmission such as the uptake rate of dopamine and neurotransmitter released per stimulus pulse. The rate of uptake can be related to the rate at which the dopamine transporter is functioning as well as the total number of transporters in a given location. The use of FSCV is sub-optimal for this task however, since adsorption decreases the observed uptake rate [2]. Oxidation of dopamine with constant-potential amperometry occurs without adsorption which significantly improves the accuracy of observed uptake rates [5].

For quantification of factors involved in dopamine release and uptake, a diffusion-based modeling program was employed [6]. The program can only evaluate amperometry data since it is unable to compensate for adsorption. The program employs a finite difference model of dopamine diffusion in which tortuosity is accounted for by a diminished value of the diffusion coefficient relative to its value in solution. Release is considered to be instantaneous and clearance is modeled by Michaelis-Menten kinetics. The Michaelis-Menten model is appropriate since dopamine taken up into the cell by the transporter generates concentration decreases that mimic enzymatic degradation [7]. A best-fit with experimental data is performed by manipulation of the dopamine released per pulse ($[DA]_p$), maximum rate of uptake (V_{max}), and dopamine's affinity for the transporter (K_m). Under normal conditions, K_m is set to a value determined in isolated tissue, 0.2 μM , and V_{max} , which is dependent upon the density of transporters, is varied to provide a best fit [8, 9].

Principle component regression

In freely-moving experiments, changes in dopamine concentrations often occur simultaneously with changes in pH. Dopamine concentrations in freely-moving experiments are therefore obtained with a principle component regression (PCR) program capable of separating the two signals [10]. A training set with several cyclic voltammograms of different concentrations of dopamine and pH changes was obtained through application of a range of stimulation pulses and currents in vivo. All files analyzed with PCR used the minimum number of factors required to reach 95% confidence. Electrodes were calibrated post-experiment with a range of dopamine concentrations from 100 nM to 1 μ M to obtain scaling factors.

ELECTROPHYSIOLOGY

A variety of techniques have emerged allowing everything from the measurement of the potential of entire neurons to the conductance of a single ion channel to be recorded. Many techniques, such as current and voltage clamp and patch clamp, require physical contact between the electrode and cell being measured. These techniques are rarely used in awake animal preparations because of the technical difficulty of securing and holding a neuron with an electrophysiological electrode. However, extracellular recordings can be readily made in freely moving animals. This recording technique does not require visible location of the target neuron nor physical contact to measure neural activity. Rather, the electrode measures voltage fluctuations occurring during action potential generation at the cell body of neurons. Upon depolarization, the influx of sodium into the cell appears as a decrease in measured potential of the extracellular fluid

while flow of potassium during the return to the resting potential creates a brief increase in voltage. The size and shape of the voltage waveform conveys information about the type of neuron being sampled and the distance between the electrode and neuron. Once a waveform is isolated from the background noise, the frequency of action potential events may be correlated to drug administration and behavioral events.

Electrophysiological recordings employed the same carbon-fiber electrodes used for electrochemistry. The extracellular recordings were filtered using an external band-pass filter (Krohn-Hite, Brockton, MA) set to accept frequencies from 300 to 30,000 Hz. Characteristic action potentials were selected using both online (Sort Client, Plexon Inc, Dallas, TX) and offline sorting (Offline Sorter, Plexon Inc, Dallas, TX) programs and analyzed with Neuroexplorer software (Plexon Inc, Dallas, TX). Electrophysiology data is graphed using perievent raster plots in which the frequency of action potential events is calculated over a short time period. The time periods, known as bins, are displayed sequentially for the experiment.

In addition to traditional electrophysiological recordings, experiments using the combined electrophysiology and FSCV technique were also performed. The technique uses the time between waveform applications to record electrophysiological data [11]. This is achieved by activating a switch on the headstage to change between a current follower circuit for FSCV and a voltage follower circuit for electrophysiology. The combined technique requires application of the triangle waveform at 5 Hz with the first 50 points of the waveform removed from data collection due to glitches generated by switching. A negative holding voltage is not applied to the electrode with the combined

technique. The resulting decrease in adsorption decreases FSCV's sensitivity for catecholamines.

INJECTIONS

Systemic injection was used for all drugs of abuse and some antagonists. All drugs injected systemically were dissolved in 0.9% w/v sodium chloride solution. For anesthetized experiments, i.p. injections were performed. Freely moving experiments were performed using animals with an implanted jugular vein catheter through which i.v. administration of drug solutions were applied.

Providing an intermediate level of spatial selectivity, microinjection injects compounds in large enough quantities to affect a region of the rat brain [12]. Performed by injecting drug solution directly into the brain into the region of interest, the technique circumvents the blood/brain barrier and allows injection of otherwise toxic compounds. Microinjection into the VTA was performed using a combined microinjection/stimulation probe. Proper placement was verified by the presence of stimulated dopamine release. Confirmation of successful injection requires either a robust behavioral effect or modulation of dopamine release or cell firing rates.

Iontophoresis

Iontophoresis was performed using a multi-channel Neurophore iontophoresis pump (Harvard Apparatus, Holliston, MA). Iontophoresis probes were constructed from either two or four barrel micro capillary tubes, with one barrel containing the carbon-fiber microelectrode. A current return (also called a balance barrel) is required to complete the

circuit for iontophoresis. With 2-barrel probes, a silver wire serving as an external current return was placed in the brain contralateral to the iontophoresis probe. With 4 barrel probes, one barrel was filled with 250 mM NaCl to serve as the current return. Ejection currents between 5 and 200 nA were used. A SEM image of a 4-barrel iontophoresis probe is shown in **Figure 2.3**. Diffusion of drug from the barrels was controlled with 10 nA attractive retaining current application between ejections.

The characteristics of iontophoretic ejection were examined before *in vivo* use began. Previous tests found iontophoresis was highly variable from electrode to electrode, leading to great uncertainty about the amount ejected [12, 13]. Dopamine was chosen as the test molecule since FSCV detection of the catecholamine is well characterized. Initial *in vitro* tests were performed with 2-barrel iontophoresis probes in HEPES buffer. The results of two tests exploring general iontophoresis ejection characteristics are displayed in **Figure 2.4**. As shown in panel A, numerous ejections from the same electrode were found to be very consistent provided the retaining current and length of time between ejections was constant. The ejection efficiency, or amount of dopamine ejected at a given current, was found to vary by as much as an order of magnitude across electrodes as shown in panel B. Similar results were found by Millar et al. previously [14].

The degree of spatial localization of iontophoresis ejections was determined in mouse brain slices and the anesthetized rat. For the brain slice experiment, an iontophoresis probe was lowered into the caudate-putamen and a second carbon-fiber microelectrode was placed in the same plane a known distance from the iontophoresis probe. The concentration of dopamine released by iontophoretic ejection was measured

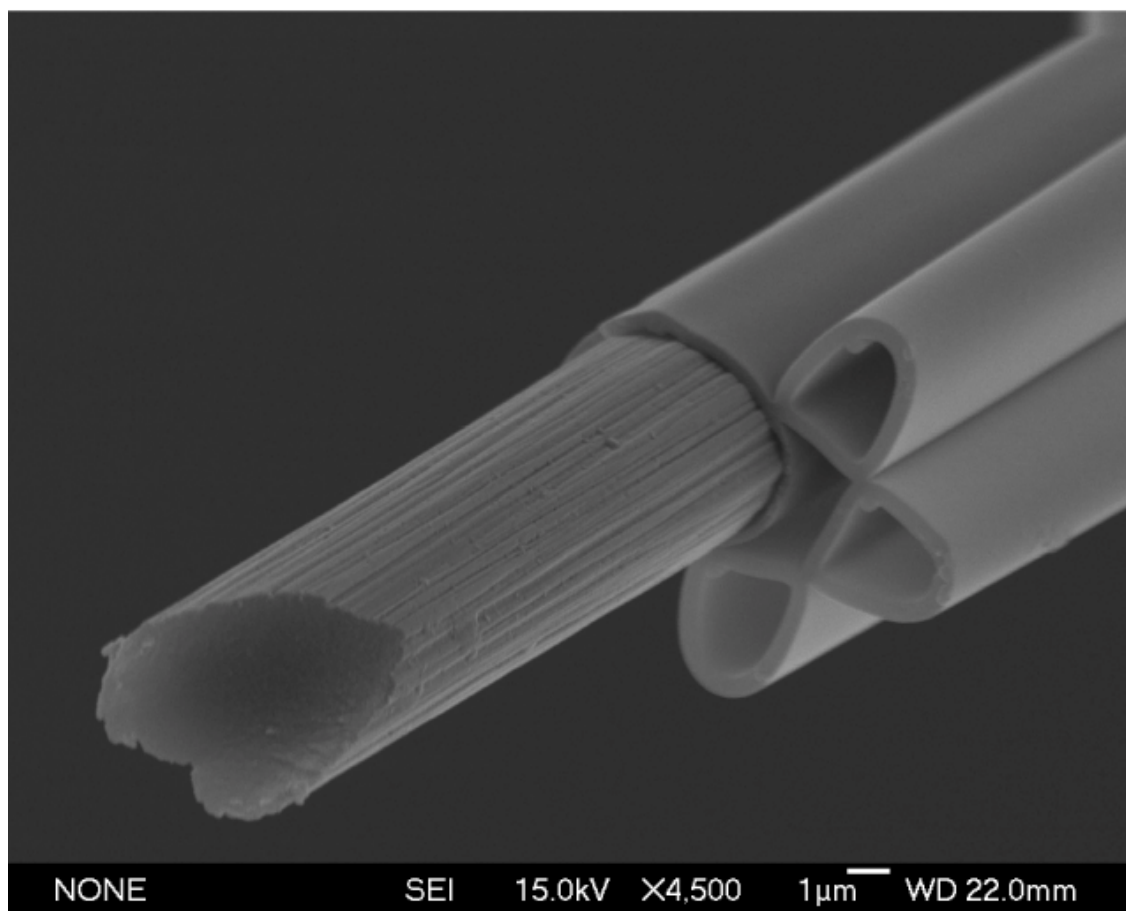


Figure 2.3: Image of 4-barrel iontophoresis probe. A SEM of an iontophoresis probe constructed with a T-650 carbon fiber in a 4-barrel microcapillary tube.

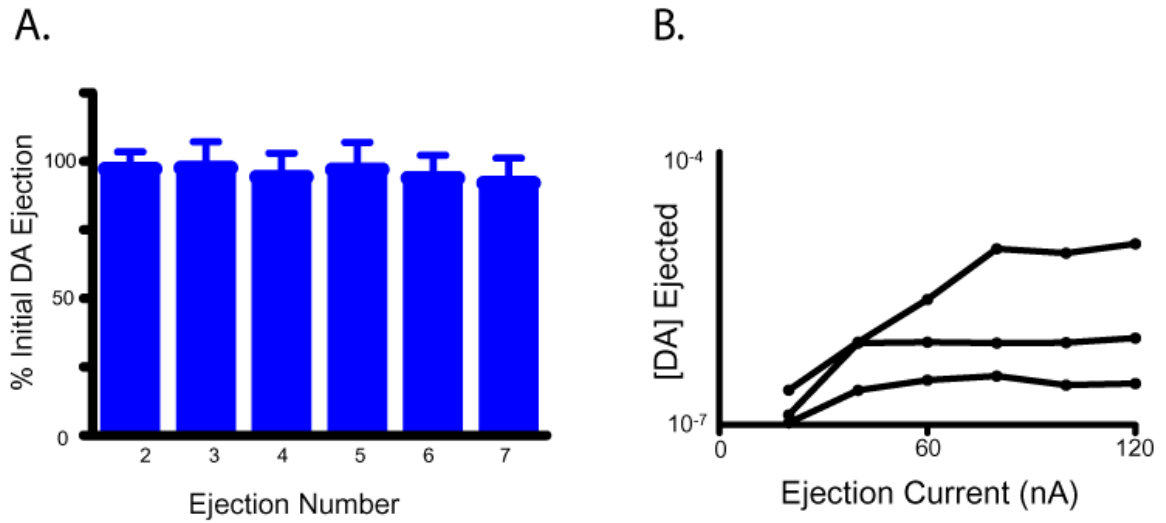


Figure 2.4: Ejection characteristics of iontophoresis probes. **A)** Ejection precision for dopamine iontophoresis in vitro. Maximum dopamine concentrations from seven successive 10 second dopamine ejections were normalized to the initial injection ($n = 5$). Ejections were spaced 30 s apart and a -10 nA retaining current was applied between ejections. Error bars display the standard deviation. **B)** Ejection efficiency for three different iontophoresis probes. Concentrations are the maximum dopamine concentration produced by a 10 second ejection at various ejection currents.

at both probes at multiple separation distances from 10 μm to 100 μm . The concentration of dopamine at the second probe was greatly diminished at just 10 μm separation and barely detectable at 100 μm . **Figure 2.5** displays the dopamine concentrations detected at distances of only 10 and 20 μm from the point of ejection.

The anesthetized experiment used quinpirole, a D2 agonist that mimics the presence of dopamine at D2 autoreceptors but is not cleared via the dopamine transporter or enzymatic degradation like the endogenous transmitter. Quinpirole was ejected for 15 minutes at 20-40 nA at a given location. At each location, dopamine release was greatly decreased and failed to recover within 15 minutes after cessation of quinpirole ejection. When the electrode was moved a depth of 200-500 μm , dopamine release was near predrug levels and fully responsive to quinpirole. The traces of individual release events at various depths are in **Figure 2.6**. This finding suggests that diffusion alone was enough to limit iontophoresis' radius of impact to just a few hundred microns even for long ejections.

CONCLUSION

The carbon-fiber electrode provides a platform for electrochemical detection and extra-cellular unit recordings, enabling dopamine concentration measurements with varying time resolution and selectivity and monitoring changes in post-synaptic neuronal activity. Through the use different drug delivery techniques, the required level of spatial resolution and behavioral modification can be obtained. Through application of the various techniques described here, a series of experiments ranging from measuring the

basal dopamine level to obtaining the effect of dopamine receptors on cell activity in a freely-moving rat were possible.

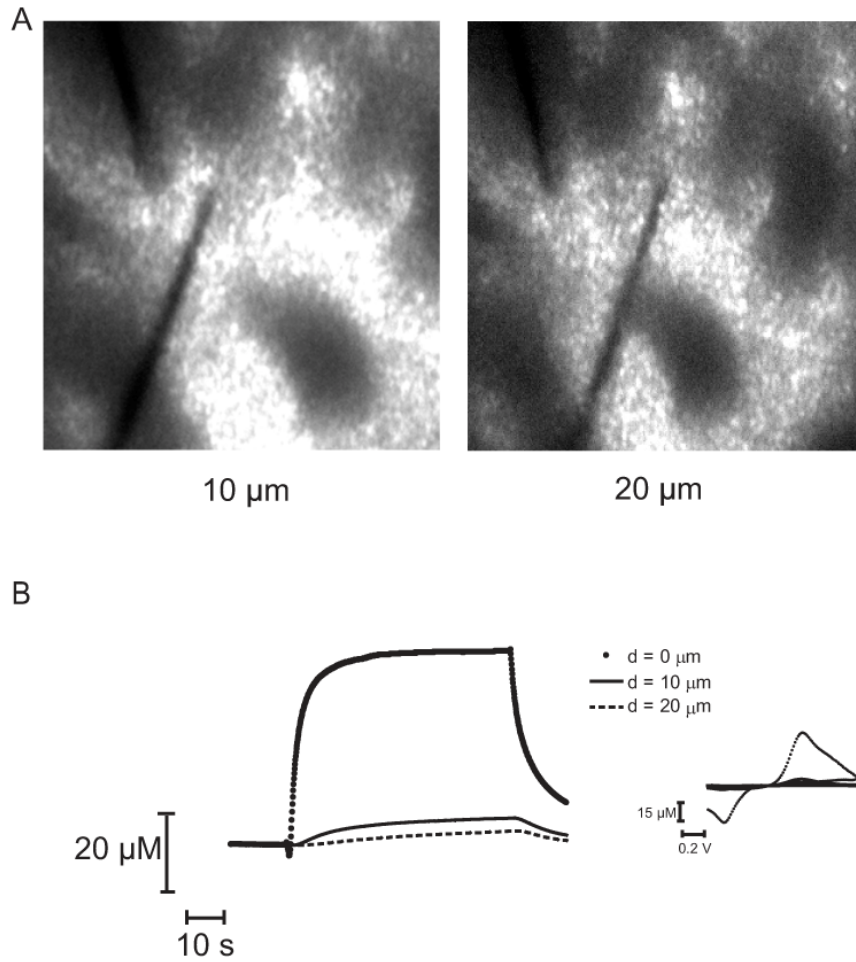


Figure 2.5: Localization of iontophoresis in vitro. **A)** Photos of the confocal image of the iontophoresis electrode and single-barrel electrode within the mouse striatum. The left panel shows the electrodes at a 10 μm separation and the right panel at 20 μm . **B)** The concentrations of ejected dopamine detected at the iontophoresis electrode and at the second electrode at 10 and 20 μm separation.

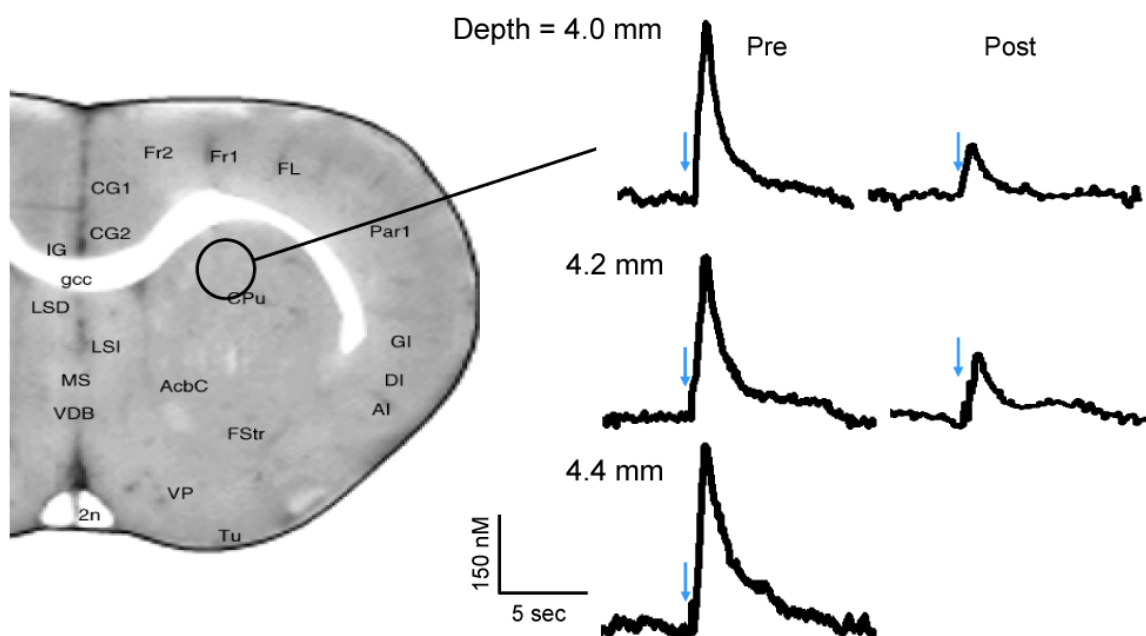


Figure 2.6: Localization of iontophoresis ejection in vivo. Left: A labeled picture of a coronal rat brain slice of the sampled region. All three recording sites occurred within a region similar to the area circled. Right: Traces labeled Pre are the average of 10 pre-drug stimulations at three different depths. Traces labeled post are the average of 10 stimulations collected after 15 minutes of continuous quinpirole ejection. Blue arrows denote the initiation of the stimulus train which consisted of 40 pulses at 60 Hz and 300 μ A. All stimulations occurred at one minute intervals.

REFERENCES

1. Peters, J.L., et al., *Ultrastructure at carbon fiber microelectrode implantation sites after acute voltammetric measurements in the striatum of anesthetized rats*. J Neurosci Methods, 2004. **137**(1): p. 9-23.
2. Bath, B.D., et al., *Subsecond adsorption and desorption of dopamine at carbon-fiber microelectrodes*. Anal Chem, 2000. **72**(24): p. 5994-6002.
3. Heien, M.L., et al., *Overoxidation of carbon-fiber microelectrodes enhances dopamine adsorption and increases sensitivity*. Analyst, 2003. **128**(12): p. 1413-9.
4. Michael, D.J. and R.M. Wightman, *Electrochemical monitoring of biogenic amine neurotransmission in real time*. J Pharm Biomed Anal, 1999. **19**(1-2): p. 33-46.
5. Venton, B.J., K.P. Troyer, and R.M. Wightman, *Response times of carbon fiber microelectrodes to dynamic changes in catecholamine concentration*. Anal Chem, 2002. **74**(3): p. 539-46.
6. Schonfuss, D., et al., *Modelling constant potential amperometry for investigations of dopaminergic neurotransmission kinetics in vivo*. J Neurosci Methods, 2001. **112**(2): p. 163-72.
7. Wightman, R.M., et al., *Real-time characterization of dopamine overflow and uptake in the rat striatum*. Neuroscience, 1988. **25**(2): p. 513-23.
8. Joseph, J.D., et al., *Dopamine autoreceptor regulation of release and uptake in mouse brain slices in the absence of D(3) receptors*. Neuroscience, 2002. **112**(1): p. 39-49.
9. Ross, S.B., *Synaptic concentration of dopamine in the mouse striatum in relationship to the kinetic properties of the dopamine receptors and uptake mechanism*. J Neurochem, 1991. **56**(1): p. 22-9.
10. Heien, M.L., M.A. Johnson, and R.M. Wightman, *Resolving neurotransmitters detected by fast-scan cyclic voltammetry*. Anal Chem, 2004. **76**(19): p. 5697-704.
11. Cheer, J.F., et al., *Simultaneous dopamine and single-unit recordings reveal accumbens GABAergic responses: implications for intracranial self-stimulation*. Proc Natl Acad Sci U S A, 2005. **102**(52): p. 19150-5.
12. Hicks, T.P., *The history and development of microiontophoresis in experimental neurobiology*. Prog Neurobiol, 1984. **22**(3): p. 185-240.

13. Armstrong-James, M., J. Millar, and Z.L. Kruk, *Quantification of noradrenaline iontophoresis*. Nature, 1980. **288**(5787): p. 181-3.
14. Armstrong-James, M., et al., *Quantitative iontophoresis of catecholamines using multibarrel carbon fibre microelectrodes*. J Neurosci Methods, 1981. **4**(4): p. 385-406.

CHAPTER 3

IONTOPHORESIS IN THE BRAIN OF ANESTHETIZED RATS

INTRODUCTION

The simplified view of neurochemical signaling is that neurotransmitters released by a presynaptic process only interact with receptors on a second, post-synaptic neuron. However, the released neurotransmitter can also interact with the neuron that released it through autoreceptors. In addition, other neurotransmitters can modulate the release of the primary neurotransmitter of interest. In this chapter, some of these actions are studied for the dopamine neurotransmitter system in the caudate nucleus using the combined use of fast-scan cyclic voltammetry, electrophysiology, and iontophoresis.

The D2 receptor is expressed pre-synaptically on dopamine neurons throughout the striatum. Termed autoinhibition because the neuron modulates its own release, activation of the receptor initiates a signaling cascade that leads to a decrease in calcium conductance and down-regulation of tyrosine hydroxylase [1-4], the rate-limiting step in dopamine synthesis. The inhibition of individual dopamine release events is estimated to have an effect within a window between 200 ms and 5 s [5, 6].

Glutamate neurons from numerous brain regions also have inputs into the striatum [7]. Glutamate and dopamine effects are strongly linked because they frequently form synapses on the same neurons [8]. Studies with intracellular recording techniques have shown that dopamine can inhibit glutamate release [9, 10]. In addition, glutamate has been shown to inhibit stimulated dopamine release from cultured cells and in brain slices [11-13]. The inhibition in cultured neurons displayed a dependence upon mGluR5 receptors [13]. In brain slices, the effect appears to be due to NMDA receptors [12], even

though ionotropic glutamate receptors may not be expressed on dopamine terminals. Considerable evidence indicates that activation of NMDA receptors on nondopaminergic cells increases H_2O_2 production, which in turn activates ATP-sensitive potassium channels that decrease dopamine release [14, 15].

The effect of dopamine release upon the activity of medium spiny neurons (MSNs), the neurons with which dopamine neurons form synapses, is also an area of current investigation [16]. MSNs may express both D1 and D2 dopamine receptors although, in the striatum, the majority express one or the other [17]. The activation of D1 receptors triggers a signaling cascade that leads to increased phosphorylation of DARP-32 and increases the activity of the neuron [18]. The D2 receptor plays an opposing role, decreasing phosphorylation of DARP-32 and decreasing activity. The fact dopamine and glutamate both target MSNs has led to the hypothesis that dopamine modulates glutamate signaling. Electrophysiology experiments suggest dopamine acts as a filter for glutamate signals by increasing the MSNs responsiveness to strong signals while decreasing the responsiveness to weak signals [19, 20]. The net effect is an increase in the signal to noise of MSN activity.

With the complexity of dopamine's role and dependence upon glutamatergic inputs, the electrophysiological study of the effects of dopamine release upon MSN firing produced a wide range of results [21]. Further complicated by a relatively slow timescale for effects when compared to fast neurotransmitters such as glutamate, interpretation of results has often been difficult [22]. Previous investigations have shown two distinct responses of MSNs from stimulation of dopamine inputs, with the rapid effects due to co-stimulation of glutamatergic inputs and the second, prolonged effect dopaminergic in

nature [23]. Other studies using stimulations obtained a dual effect from dopamine, with low concentrations producing excitations and high concentrations inhibitions [20, 24].

In order to investigate dopamine neurotransmission in anesthetized animals, an iontophoresis probe containing a carbon-fiber microelectrode was employed. Stimulated dopamine release was modulated by ejection of glutamate and the D2 receptor agonist, quinpirole. The impact of dopamine upon MSN activity for glutamate-excited cells was also investigated.

METHODS

Male Sprague-Dawley rats weighing between 300-400 g were anesthetized using urethane (1.5 g/kg). The rats were secured in a stereotaxic apparatus and holes were drilled for the stimulation electrode (+0.8 mm ML, -5.3 mm AP) and working electrode (+2.0 mm ML, +1.2 mm AP). A silver/silver chloride reference electrode was implanted contralateral to the stimulating electrode. The stimulating electrode was lowered to 8.5 mm depth to activate the VTA/MFB. The working electrode was lowered to an initial depth of 5.0 mm for measurements in the striatum.

Electrodes used were constructed from either 2 or 4-barrel microcapillary tubes. Both types of electrodes were fabricated by loading one barrel with a T-650 carbon fiber and pulling the capillary tube in a vertical pipette puller in which a tight glass seal was formed to the carbon fiber while the barrels not containing the carbon fiber each formed a narrow opening ($< 10\ \mu\text{m}$ diameter). The carbon fibers were cut to between 30 – 50 μm in length. With 4-barrel electrodes, one barrel was filled with 250 mM NaCl solution and

used as the current return. In experiments using 2-barrel electrodes, a silver wire was inserted into the tissue to act as a current return.

Dopamine was detected with FSCV using the triangle waveform scanning from -0.4 V to 1.3 V and back to -0.4 V at 400 V/s. For stimulated dopamine release studies, the maximum release generated from 300 μ A, 40 pulse stimulations of the MFB was recorded. Stimulations were applied every 60 seconds. A minimum of 10 stimulations were performed at each location to ensure stable release before iontophoresis applications were initiated. Iontophoretic ejection of agonists and antagonists was performed continuously for 15 stimulations. Fifteen recovery file stimulations were recorded after the final drug application at each site. Multiple recording sites in the caudate-putamen at least 300 μ m apart and located between 5 mm and 8 mm depth were used in each animal.

External unit recordings employed the same carbon-fiber electrodes used for electrochemistry. The extracellular recordings were filtered using an external band-pass filter (Krohn-Hite, Brockton, MA) set to accept frequencies from 300 to 3,000 Hz. Characteristic action potentials were selected using both online (Sort Client, Plexon Inc, Dallas, TX) and offline (Offline Sorter, Plexon Inc, Dallas, TX) sorting programs and analyzed with Neuroexplorer (Plexon Inc, Dallas, TX) software.

For electrophysiology experiments, a four-barrel iontophoresis probe was lowered to an initial depth of 4 mm. The drug barrels contained 250 mM glutamic acid dissolved in DI water and either 10 mM dopamine HCl or 10 mM 6-cyano-7-nitroquinoxaline-2,3-dione (CNQX) in DI water. Neurons were isolated by slowly lowering the electrode with a low glutamate ejection current (-5 nA). Once isolated, ten files were collected at one minute intervals. Dopamine or CNQX was ejected for 20 seconds. A separate set of files

was obtained for dopamine ejection at a low and high ejection current.

Electrophysiological recordings also containing voltammetric detection of dopamine were collected using the combined technique [25]. The combined technique uses the period between waveform applications to record electrophysiology data. Dopamine ejection was quantified using the intermediate waveform with the cyclic voltammetry waveform applied at 5 Hz. Once collected, all firing patterns were sorted and time-locked to the initiation of ejection.

For quinpirole ejection experiments, 4-barrel microcapillary tubes were used to produce a probe containing a carbon-fiber microelectrode, a balance barrel (250 mM NaCl) and two drug barrels. Quinpirole HCl (10 mM, pH = 4) was loaded into the first barrel and raclopride HCl (10 mM in deionized water) in the second. A -10 nA retaining current and ejection currents between +10 and +150 nA were used for both compounds. Probes in systemic raclopride administration experiments were two-barrel microcapillary tubes with a carbon-fiber microelectrode and quinpirole drug barrel. Electrodes for both experiments were loaded with drug solution at least 20 minutes prior to the experiment to ensure air bubbles did not block ejection. Raclopride for systemic injection (1 mg/kg in saline) was introduced via i.p. injection. Glutamate ejection experiments followed the same design as the quinpirole experiments. Iontophoretic ejection of glutamic acid (250 mM in DI water) was performed at low ejection currents (-5 to -40 nA) with a +10 nA retaining current applied when not ejecting.

All chemicals were obtained from Sigma-Aldrich (St. Louis, MO) and used as delivered. Capillaries were purchased from A-M systems (Carlsborg, WA) for 2-barrel capillaries and Stoelting Instrument Co. (Chicago, IL) for 4-barrel capillaries.

RESULTS

Glutamate and dopamine effects on single unit activity

In the anesthetized preparation, active units are rarely seen in the dorsal striatum. To evoke unit activity for the electrophysiology study, glutamate was ejected continuously. Isolation of several cells on a single track was often obtained with this method. The firing pattern of cells in the striatum in the presence of glutamate was characterized as highly burst-oriented. Single action potentials were rarely generated. Instead short duration, high frequency bursts with fairly long inter-burst time intervals were observed. **Figure 3.1** shows the successful inhibition of the glutamate excitation with co-ejection of the AMPA receptor antagonist, CNQX (n=3). Co-ejection of dopamine drastically decreased the activity of most cells. Of the cells recorded, dopamine inhibited the firing rates of 43% (9 out of 21). Of the nine inhibited cells, 5 displayed a 2-state response to dopamine ejections with multiple cells responsive to only the higher ejection current as shown in **Figure 3.2**. Cells inhibited by both ejection currents failed to show a difference in the magnitude of firing rate decrease. For the ejection of glutamate, CNQX, and dopamine, effects upon cell firing occurred within seconds of the initiation of the ejection current. Ejection durations of 20 seconds were sufficient to characterize the impact of the iontophoretic ejection of these compounds upon cell activity.

Glutamate effects on stimulated dopamine release

Glutamate ejection was found to strongly inhibit stimulated dopamine release in a dose dependent manner (**Figure 3.3**). Glutamate ejection produced an average inhibition

compared to pre-drug stimulated release of $63 \pm 4\%$ ($n = 12$) at -20 or -40 nA ejection currents. The ejection of glutamate for durations comparable to those required to modulate cell firing was insufficient to inhibit stimulated dopamine release. Instead, continuous ejection over several minutes was necessary to obtain the maximum effect.

Effect of dopaminergic agents on dopamine release

The D2 agonist quinpirole was applied with iontophoresis and inhibited stimulated dopamine release. A representative trial showing quinpirole inhibition along with traces of individual release events is shown in panels A and B of **Figure 3.4**. As with glutamate ejection, a continuous ejection of several minutes was required to generate a significant change in dopamine release, with the maximum drug effect occurring after approximately 10 minutes. At different sites within the dorsal striatum, a range of quinpirole ejections were performed that displayed a dose-dependent decrease in stimulated dopamine release as shown in panel C, **Figure 3.4**. The average maximum inhibition was $77 \pm 3\%$ for an ejection currents of 20-40 nA ($n = 10$).

Attempts to block the quinpirole inhibition were performed by iontophoretically ejecting raclopride, a D2 antagonist, continuously for 15 minutes before co-ejecting both drugs while stimulating dopamine neurons. Raclopride was ejected before quinpirole in order to lessen the potential effect of differing ejection efficiencies. The results of raclopride ejection were highly erratic, however. As shown in the “Iontophoresis” panel in **Figure 3.5**, rather than increasing stimulated dopamine release as hypothesized, raclopride would often inhibit dopamine release. It is unlikely that application of the ejection current to the raclopride barrel was also causing ejection from the quinpirole

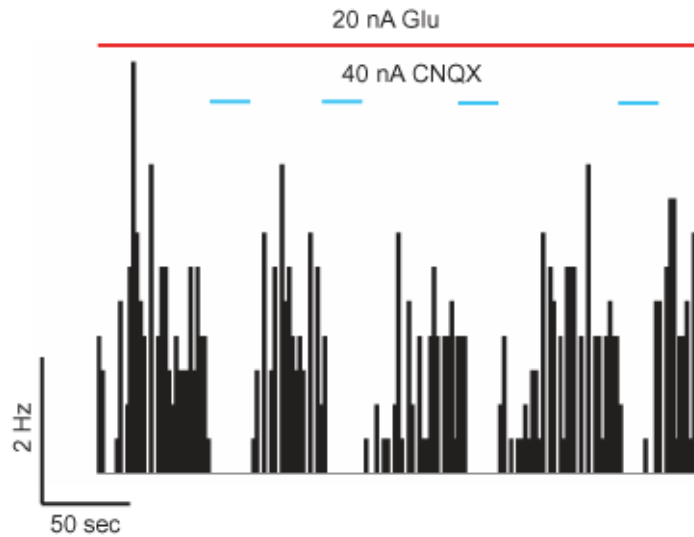


Figure 3.1: The effect of glutamate iontophoresis upon cell activity. The red line indicates continuous glutamate ejection to activate an otherwise inactive neuron. Blue dashes indicate ejection of the AMPA receptor antagonist, CNQX. Ejection of CNQX decreased the cell's response to glutamate iontophoresis. Similar results were obtained in 3 animals.

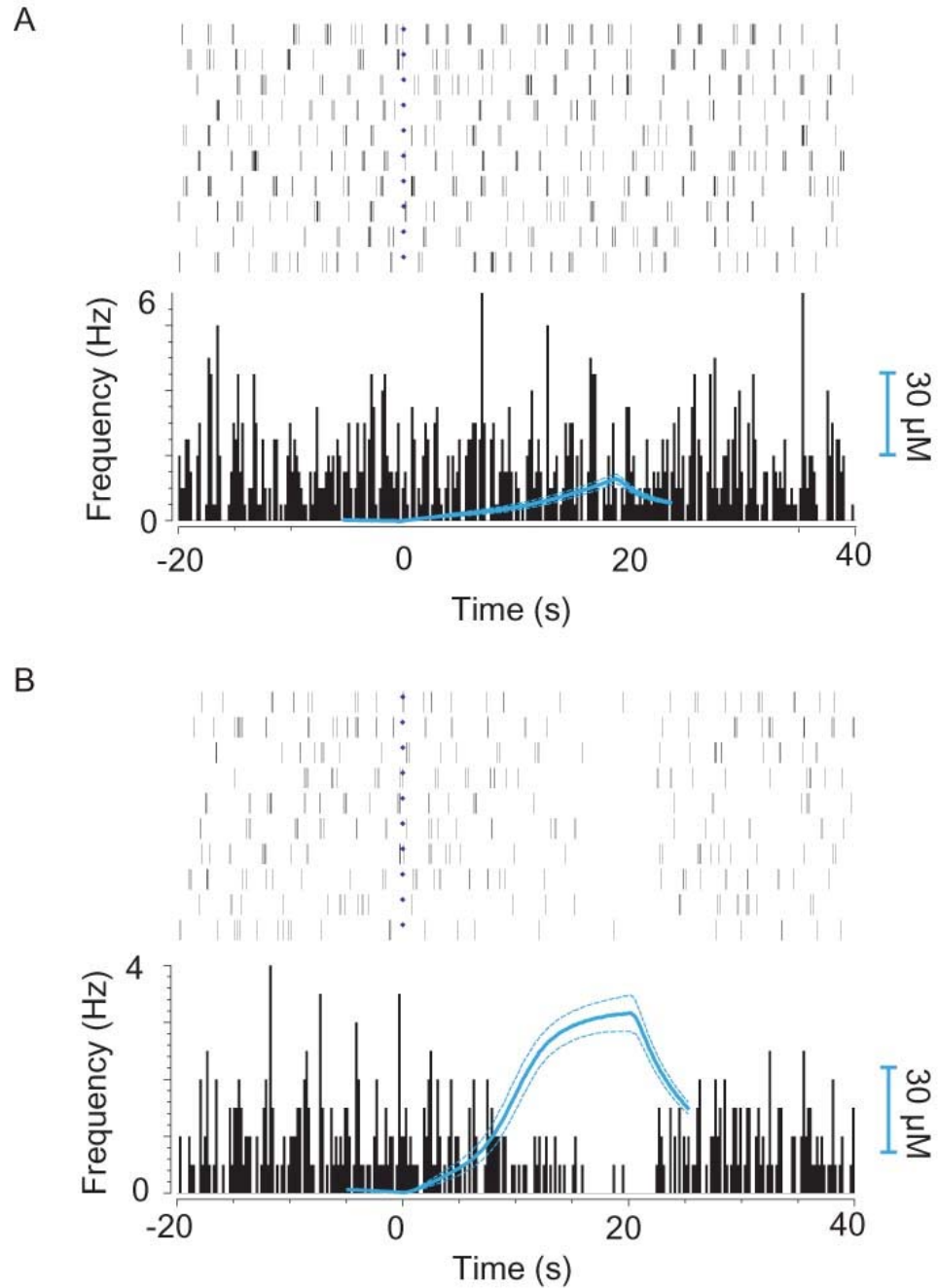


Figure 3.2: Effect of dopamine iontophoresis upon glutamate-excited cell activity. **A)** The periavent raster of a cell excited by -5 nA continuous glutamate ejection. The blue line indicates the dopamine released by a 20 seconds of 5 nA dopamine ejection. **B)** The periavent histogram of the same cell with the blue line indicating the dopamine released by a 20 second, 15 nA dopamine ejection. Ten trials were performed at each dopamine ejection current

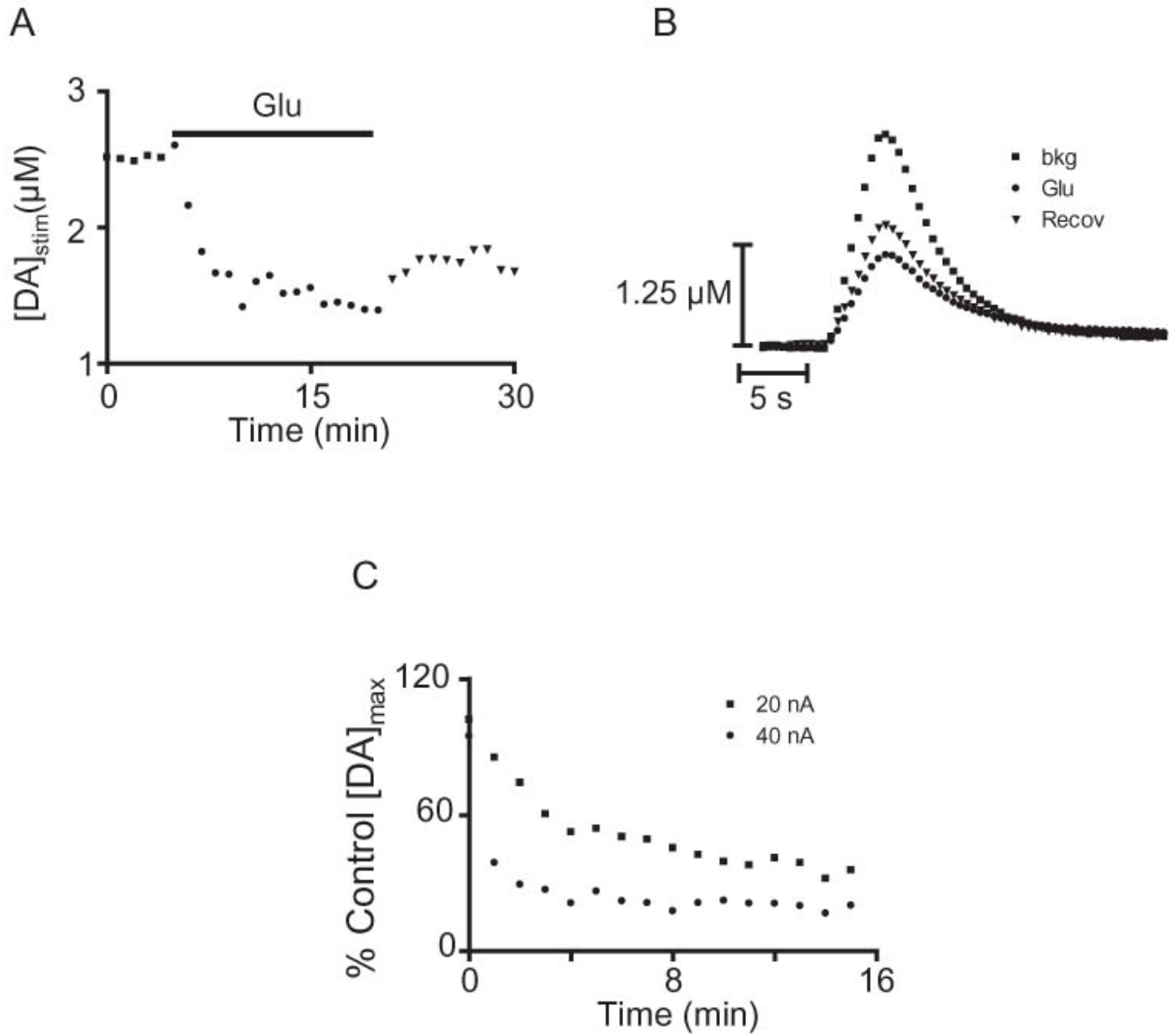


Figure 3.3: The effect of glutamate iontophoresis upon stimulated dopamine release.

A) The maximum stimulated dopamine release during -20 nA glutamate ejection. **B)** Representative traces of individual stimulations before, during, and 15 minutes after glutamate ejection. **C)** The dose-response of glutamate ejection. The % inhibition of stimulated dopamine release normalized to the average pre-drug maximum release at 2 different ejection currents. Each ejection was performed at different recording locations within the same animal. All stimulations were 40 pulses at 60 Hz and 300 μA .

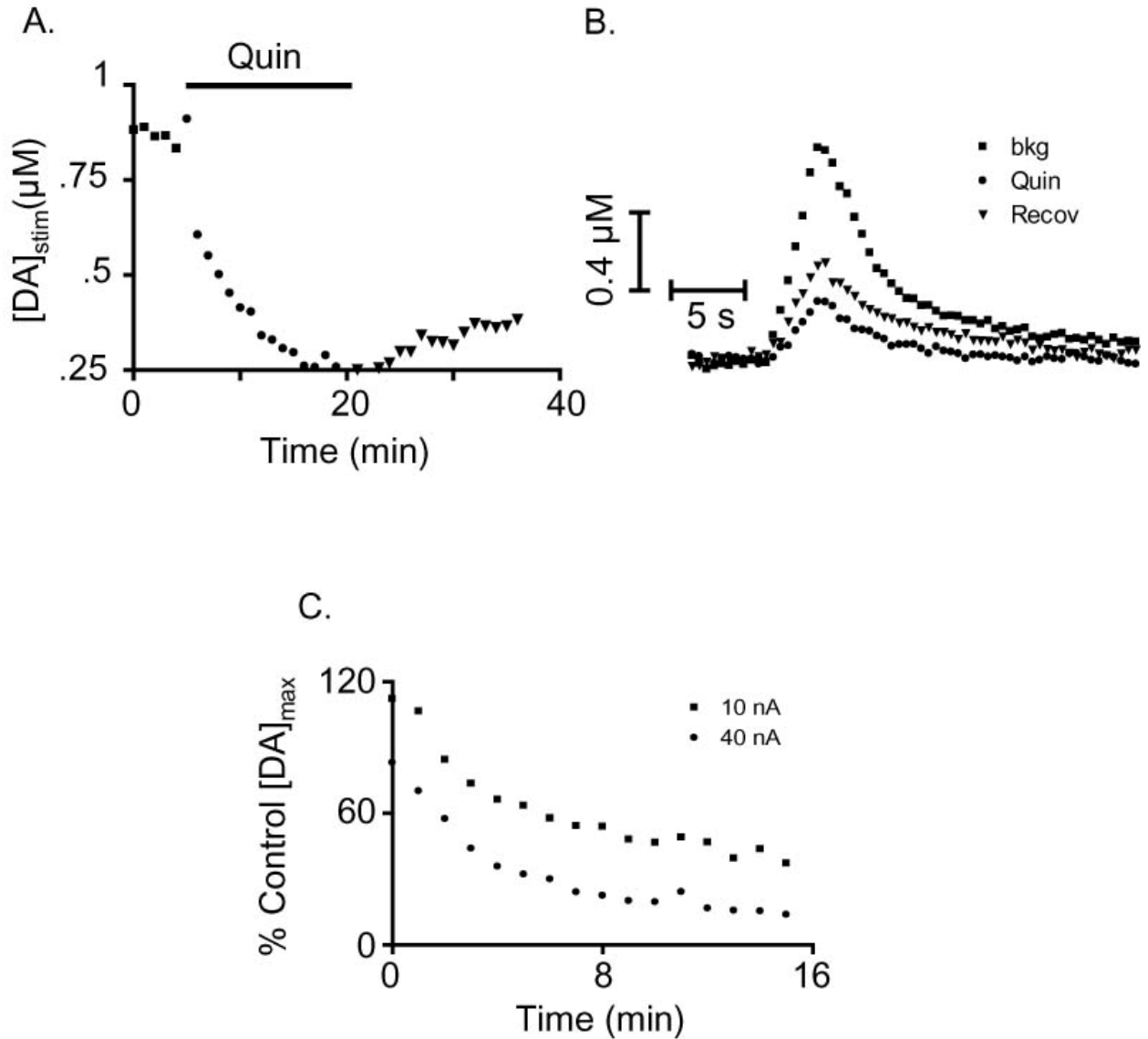


Figure 3.4: The effect of quinpirole iontophoresis upon stimulated dopamine release.

A) The maximum stimulated dopamine release during 20 nA quinpirole ejection. **B)** Representative traces of individual stimulations before, during, and 15 minutes after quinpirole ejection. **C)** The dose-response of quinpirole ejection. The % inhibition of stimulated dopamine release normalized to the average pre-drug maximum release at 3 different ejection currents. Each ejection was performed at a different recording location within the same animal. All stimulations were 40 pulses at 60 Hz and 300 μA .

barrel since this behavior was rarely witnessed in experiments with electroactive drugs. It is also unlikely that the ejection current was triggering the inhibition because control tests using ejection of saline displayed no significant effects upon dopamine release even at high currents. The “Systemic Injection” panel shows the effect of i.p. raclopride administration within the same animal. While introduction of raclopride with iontophoresis produced contradictory results, systemic injection produced a consistent increase in stimulated dopamine release.

Systemic application of raclopride

The effect of systemic application of raclopride upon the inhibition of stimulated dopamine release from quinpirole iontophoresis was also investigated (**Figure 3.6**). The inhibition generated from quinpirole at a low ejection current (10 - 40 nA) was obtained after which the probe was moved to a drug-naïve site. At the second recording location, release was measured for 15 minutes after raclopride was injected i.p., during which stimulated dopamine release increased to between 100-400% of the predrug signal. Quinpirole was then ejected with iontophoresis at the same current as applied at the previous recording site. Quinpirole displayed a potent inhibition of dopamine release in the presence of raclopride as shown in panel C of **Figure 3.6**.

DISCUSSION

The results of this work indicate that the combined use of fast-scan cyclic voltammetry with iontophoresis is an important tool to probe neurochemical interactions.

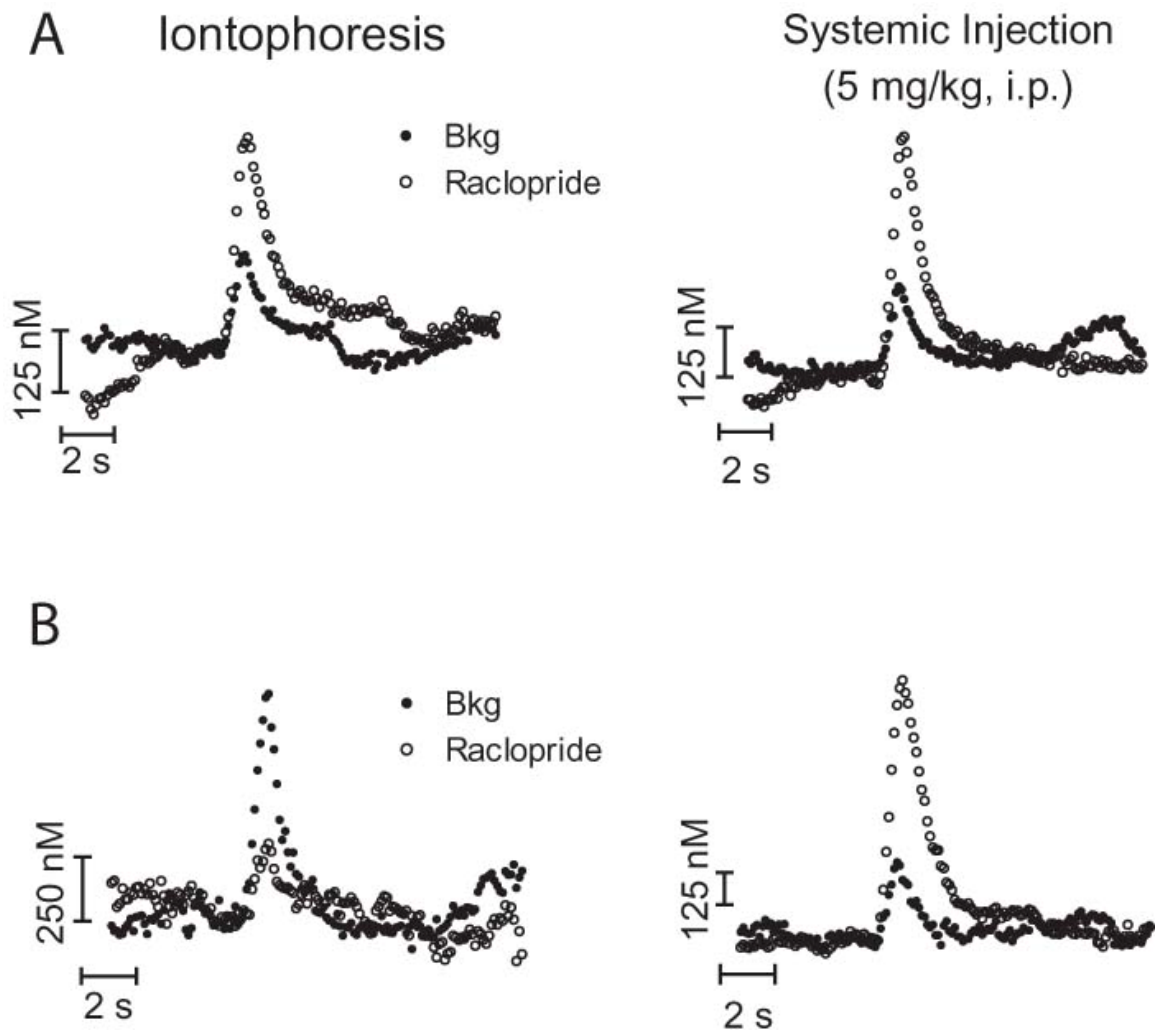


Figure 3.5: The effect of raclopride administration upon stimulated dopamine release. A) The left side shows an increase in stimulated dopamine release in response to raclopride iontophoresis. The right side shows the change generated by systemic raclopride injection at a different location within the same animal. B) The left side shows a decrease in dopamine release in response to raclopride iontophoresis. The right side is the increase in dopamine in response to systemic raclopride in the same animal.

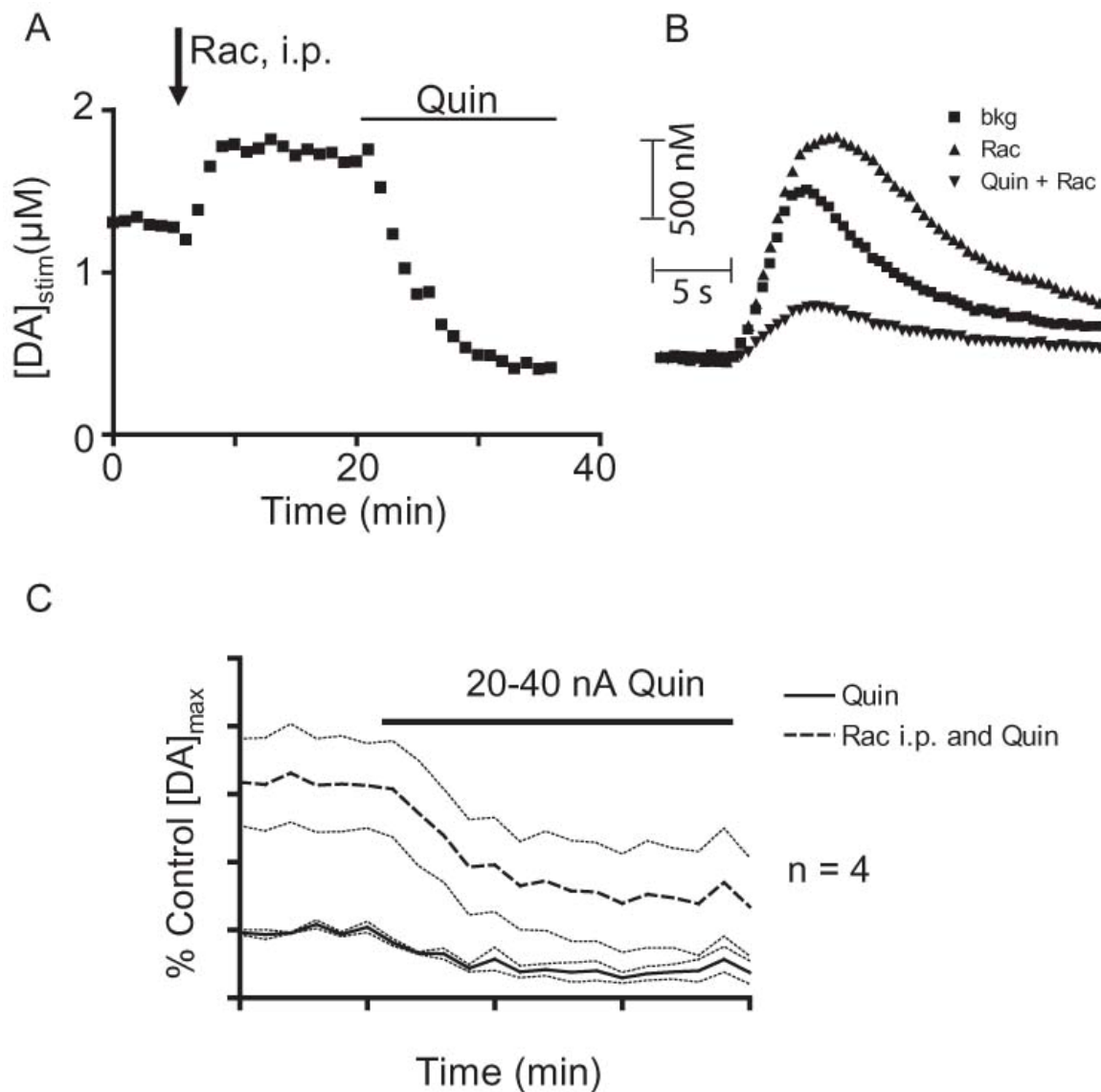


Figure 3.6: The effect of systemic raclopride on quinpirole inhibition. **A)** Maximum stimulated dopamine release following i.p. injection of 10 mg/kg raclopride and 20 nA quinpirole ejection. **B)** Representative traces from pre-drug, post-raclopride, and during quinpirole ejection stimulations. **C)** The % inhibition of dopamine release by quinpirole pre-raclopride (normalized to pre-drug dopamine release) and post-raclopride (normalized to post-raclopride dopamine release). All traces were collected at different recording sites within the same animal. All stimulations were 40 pulse, 60 Hz at 300 μA .

Fast scan cyclic voltammetry enables the concentration of electroactive species in the brain to be monitored on a subsecond time scale. Iontophoresis enables the local application of drugs into the brain directly at the measurement site, also bypassing the blood/brain barrier and minimizing toxicity concerns. In this study, iontophoresis was capable of exciting cell activity with glutamate and inhibiting the activity of the glutamate-excited cells through ejection of CNQX and dopamine. Iontophoresis was also used to inhibit stimulated dopamine release through the ejection of glutamate and quinpirole. The onset of excitation by glutamate occurs within seconds of initiating the ejection. Likewise, the onset of inhibition of this excitation by CNQX and dopamine occurred within a similar time. The inhibition of stimulated dopamine release by both glutamate and the D2 agonist, quinpirole required ejections of several minutes to obtain maximum effect.

The extreme difference in time observed for the onset of effects suggests this delay is not biological. The excitation of cell firing by glutamate ejection and subsequent inhibition via CNQX ejection displays the role of AMPA receptors in initiating the action potential. The AMPA receptors belong to the ionotropic class of receptors because they are directly linked to ion channels. This class of receptors produces rapid changes in cell activity and effects are observed within 100 ms of receptor activation [23]. Dopamine receptors are not linked directly to ion channels, and therefore produce changes in cell activity on a slower timescale of approximately 200 ms [23]. For the electrophysiology experiments, the delay of a few seconds from initiation of ejection to the effects upon cell activity is therefore the time required for the compound to diffuse from the ejection site to the receptors.

For the inhibition of stimulated dopamine release, the delay from ejection to the maximum effect was several minutes. While the inhibition of release by glutamate has only recently been observed, the effect of D2 activation has been studied extensively. The time required for a stimulated release event to inhibit release subsequent dopamine release events has been identified as 200 ms [5]. While the time required for diffusion from the point of ejection will produce a delayed response, the timecourse of several minutes is far greater than expected. This delay is not likely caused by a delay in quinpirole exiting the iontophoresis barrel and entering the extracellular space since glutamate ejection was shown to have a rapid effect upon cell activity, yet a similar slow effect upon stimulated release. Therefore the effect is likely due to differences in the efficiency of iontophoresis to modulate signals produced by measurement of single cell activity and dopamine release events.

Once entering the extracellular solution, compounds ejected by iontophoresis exhibit radial diffusion from a point source, which is then modified by the microstructure of the tissue [26]. This method allows for sizeable concentrations to be produced at the site of ejection with relatively few molecules being released. This results in a rapid decrease in concentration as the distance from the point of ejection increases. Once the ejection is terminated, the concentration of ejected compound rapidly dissipates due to diffusion as well. Experiments in brain slices where dopamine ejected via iontophoresis was detected by a second electrode a known distance away found the signal to be 10 times smaller just 10 μm away from the ejection site and no detectable signal at 100 μm or less from the ejection site.

In a previous study, an image of the microstructure of striatal tissue produced by immunostaining showed a disperse field of dopamine terminals intermixed with large GABA-ergic cell bodies [27]. The formation of an action potential at these GABA-ergic cell bodies is what is measured during the electrophysiological recordings. Activation of receptors upon an individual cell's dendrites and cell body increases or inhibits the frequency of action potentials depending upon the receptor targeted. The activation of all the receptors on the neuron's dendrites is not necessary. Instead, only a large enough percentage to generate an action potential was required.

The inhibition of dopamine release required the activation of receptors located throughout a diffuse field of numerous terminals. The concentrations of dopamine generated by electrical stimulation are believed to be the sum of release events from these numerous dopamine cell terminals [28]. This terminal field will encompass a volume of tissue surrounding the electrode. In order to obtain the maximum observed effect upon dopamine release, receptors on the terminals located throughout the sampled volume must be activated. The ejected compound must therefore reach terminals along the entire 50 μm length in sufficient concentration to modulate the measured dopamine signal. Therefore the volume of tissue the ejected compound must affect in sufficient concentration is based upon the size of the electrode and distance from which dopamine release can be detected. The substantial difference in the time required to produce maximal effect suggests that the volume of tissue involved in dopamine release measurements is considerably greater than the volume required to modulate single cell activity.

A sampling bias is also introduced in the electrophysiology experiments. The frequency with which spontaneously active medium spiny neurons are observed is too low for reliable study in the urethane anesthetized rat [29]. Therefore, only cells which the ejection of glutamate could excite were measured in this study. This could result in only neurons relatively close to the electrode and rapidly reached by iontophoresis being sampled.

The introduction of raclopride produced a range of results. The ejection of the D2 antagonist via iontophoresis often inhibited dopamine release. This contradicts the results obtained from systemic injection and previous microdialysis studies using reverse-dialysis to introduce the compound [30]. This may be a result of increasing the activity of inhibitory GABA interneurons that modulate dopamine cell activity through D2 receptor blockade. Nonetheless, the ejection of quinpirole was capable of significantly inhibiting stimulated dopamine release in the presence of systemic raclopride. This indicates that the resulting concentrations of iontophoretically-applied compounds throughout the terminal field being measured are sufficient to compete with a systemically introduced compound and therefore may be used in conjunction with other drug delivery techniques.

CONCLUSION

The pairing of iontophoresis with voltammetry and electrophysiology allows for local manipulation of measurements involving neurotransmitter release and cell activity. The nature of the two types of measurements produces dramatically different effects from compounds ejected via iontophoresis however. The ejection of glutamate, CNQX, and

dopamine produced changes in cell activity within seconds of initiating the ejection. The inhibition of stimulated dopamine release by glutamate and quinpirole required several minutes to reach the maximum effect. This difference is not due to the time response of the cells to receptor activation, but instead likely due to differences in the volume of tissue over which iontophoresis must saturate. Acting upon a relatively small section of tissue close to the point of ejection, changes in electrophysiological measurements occurred more rapidly than dopamine release measurements that are collected from tissue surrounding the entire length of the electrode.

REFERENCES

1. Cardozo, D.L. and B.P. Bean, *Voltage-dependent calcium channels in rat midbrain dopamine neurons: modulation by dopamine and GABAB receptors*. J Neurophysiol, 1995. **74**(3): p. 1137-48.
2. O'Hara, C.M., et al., *Inhibition of dopamine synthesis by dopamine D2 and D3 but not D4 receptors*. J Pharmacol Exp Ther, 1996. **277**(1): p. 186-92.
3. Onali, P. and M.C. Olianas, *Involvement of adenylate cyclase inhibition in dopamine autoreceptor regulation of tyrosine hydroxylase in rat nucleus accumbens*. Neurosci Lett, 1989. **102**(1): p. 91-6.
4. Lindgren, N., et al., *Dopamine D(2) receptors regulate tyrosine hydroxylase activity and phosphorylation at Ser40 in rat striatum*. Eur J Neurosci, 2001. **13**(4): p. 773-80.
5. Phillips, P.E., P.J. Hancock, and J.A. Stamford, *Time window of autoreceptor-mediated inhibition of limbic and striatal dopamine release*. Synapse, 2002. **44**(1): p. 15-22.
6. Benoit-Marand, M., E. Borrelli, and F. Gonon, *Inhibition of dopamine release via presynaptic D2 receptors: Time course and functional characteristics in vivo*. Journal of Neuroscience, 2001. **21**(23): p. 9134-9141.
7. Grace, A.A., et al., *Regulation of firing of dopaminergic neurons and control of goal-directed behaviors*. Trends Neurosci, 2007.
8. Sesack, S.R., et al., *Anatomical substrates for glutamate-dopamine interactions: evidence for specificity of connections and extrasynaptic actions*. Ann N Y Acad Sci, 2003. **1003**: p. 36-52.
9. Nicola, S.M. and R.C. Malenka, *Dopamine depresses excitatory and inhibitory synaptic transmission by distinct mechanisms in the nucleus accumbens*. J Neurosci, 1997. **17**(15): p. 5697-710.
10. Hjelmstad, G.O., *Dopamine excites nucleus accumbens neurons through the differential modulation of glutamate and GABA release*. J Neurosci, 2004. **24**(39): p. 8621-8.
11. Wu, Y., et al., *Inhibitory glutamatergic regulation of evoked dopamine release in striatum*. Neuroscience, 2000. **96**(1): p. 65-72.
12. Avshalumov, M.V., et al., *Glutamate-dependent inhibition of dopamine release in striatum is mediated by a new diffusible messenger, H2O2*. J Neurosci, 2003. **23**(7): p. 2744-50.

13. Zhang, H. and D. Sulzer, *Glutamate spillover in the striatum depresses dopaminergic transmission by activating group I metabotropic glutamate receptors*. J Neurosci, 2003. **23**(33): p. 10585-92.
14. Avshalumov, M.V., et al., *Endogenous hydrogen peroxide regulates the excitability of midbrain dopamine neurons via ATP-sensitive potassium channels*. J Neurosci, 2005. **25**(17): p. 4222-31.
15. Avshalumov, M.V. and M.E. Rice, *Activation of ATP-sensitive K⁺ (K(ATP)) channels by H₂O₂ underlies glutamate-dependent inhibition of striatal dopamine release*. Proc Natl Acad Sci U S A, 2003. **100**(20): p. 11729-34.
16. Sesack, S.R. and V.M. Pickel, *In the Rat Medial Nucleus-Accumbens, Hippocampal and Catecholaminergic Terminals Converge on Spiny Neurons and Are in Apposition to Each Other*. Brain Research, 1990. **527**(2): p. 266-279.
17. Surmeier, D.J., et al., *D1 and D2 dopamine-receptor modulation of striatal glutamatergic signaling in striatal medium spiny neurons*. Trends Neurosci, 2007. **30**(5): p. 228-35.
18. Svenningsson, P., et al., *DARPP-32: an integrator of neurotransmission*. Annu Rev Pharmacol Toxicol, 2004. **44**: p. 269-96.
19. West, A.R., et al., *Electrophysiological interactions between striatal glutamatergic and dopaminergic systems*. Ann N Y Acad Sci, 2003. **1003**: p. 53-74.
20. Kiyatkin, E.A. and G.V. Rebec, *Dopaminergic modulation of glutamate-induced excitations of neurons in the neostriatum and nucleus accumbens of awake, unrestrained rats*. J Neurophysiol, 1996. **75**(1): p. 142-53.
21. Nicola, S.M., J. Surmeier, and R.C. Malenka, *Dopaminergic modulation of neuronal excitability in the striatum and nucleus accumbens*. Annu Rev Neurosci, 2000. **23**: p. 185-215.
22. Neve, K. and R. Neve, *The Dopamine Receptors*. The Receptors. 1997.
23. Gonon, F., *Prolonged and extrasynaptic excitatory action of dopamine mediated by D1 receptors in the rat striatum in vivo*. J Neurosci, 1997. **17**(15): p. 5972-8.
24. Williams, G.V. and J. Millar, *Concentration-dependent actions of stimulated dopamine release on neuronal activity in rat striatum*. Neuroscience, 1990. **39**(1): p. 1-16.

25. Cheer, J.F., et al., *Simultaneous dopamine and single-unit recordings reveal accumbens GABAergic responses: implications for intracranial self-stimulation*. Proc Natl Acad Sci U S A, 2005. **102**(52): p. 19150-5.
26. Nicholson, C., J.M. Phillips, and A.R. Gardnermedwin, *Diffusion from an Iontophoretic Point Source in the Brain - Role of Tortuosity and Volume Fraction*. Brain Research, 1979. **169**(3): p. 580-584.
27. Wightman, R.M., et al., *Dopamine release is heterogeneous within microenvironments of the rat nucleus accumbens*. Eur J Neurosci, 2007. **26**(7): p. 2046-54.
28. Venton, B.J., et al., *Real-time decoding of dopamine concentration changes in the caudate-putamen during tonic and phasic firing*. J Neurochem, 2003. **87**(5): p. 1284-95.
29. Warenycia, M.W. and G.M. McKenzie, *Responses of striatal neurons to anesthetics and analgesics in freely moving rats*. Gen Pharmacol, 1984. **15**(6): p. 517-22.
30. You, Z.B., Y.Q. Chen, and R.A. Wise, *Dopamine and glutamate release in the nucleus accumbens and ventral tegmental area of rat following lateral hypothalamic self-stimulation*. Neuroscience, 2001. **107**(4): p. 629-639.

CHAPTER 4

IONTOPHORESIS IN FREELY MOVING RATS

INTRODUCTION

By changing a neuron's responsiveness to chemical signals from other neurotransmitters, dopamine is able to increase or decrease a target cell's activity [1, 2]. Electrophysiological recordings in the form of extracellular unit recordings have enabled monitoring cell activity within a freely-moving animal. The pattern and firing rate of the target neurons are impacted both by dopamine release and the release of other neurotransmitters such as glutamate and acetyl choline (ACh) [1, 3]. In order to discriminate between dopaminergic and non-dopaminergic effects, pharmacological agents must be administered to confirm the receptors responsible for the neural response. However, for experiments involving a specific behavior the application of pharmacological agents may impact the behavior, thus invalidating the results. Local drug delivery techniques such as iontophoresis must therefore be employed, which localize the drug to a sufficiently small region so that behavior is not modified.

Dopamine's direct involvement in rewarding behaviors was first observed in the 1950's [4]. However, the analytical tools available at the time were insufficient to adequately characterize dopamine's specific actions. After electrophysiological recording techniques improved, Wolfram Schultz showed that dopamine neurons display burst firing in response to reward-related cues [5]. This implies a role for phasic dopamine release in the reward-related behaviors, though analytical techniques were still unable to combine sufficient time resolution, selectivity and sensitivity required to

measure the dopamine fluctuations directly. Recent improvements in electrochemical detection of dopamine have allowed the detection of release events in freely-moving rats [6, 7]. As predicted by Schultz's findings, transient dopamine concentrations have been observed in several reward-related behaviors. Naturally-occurring dopamine has been observed in response to natural reward behaviors such as sucrose administration and sex behaviors [8, 9]. Within addiction models, the administration of drugs of abuse such as cocaine and cues associated with inter-cranial self-stimulation (ICSS) generate spontaneous dopamine signals as well [10, 11]. The presence of transient dopamine only provides half of the information required to understand dopamine signaling in behavior however.

Coupling electrochemistry with electrophysiology allows detection of dopamine release events as well as changes in the firing rates of nearby cells. This combination provides real-time measurement of both the chemical input signal and the electrophysiological output signal [12]. The addition of iontophoresis is required in order to confirm dopamine's role in any firing rate modifications. The experiments discussed here show the use of carbon-fiber electrodes combined with iontophoresis in behaving, freely-moving animals.

METHODS

Male Sprague-Dawley rats weighing between 300-400 g were anesthetized using ketamine (10 mg/kg) and xylazine (1 mg/kg). The rats were then secured in a stereotaxic apparatus and the stimulation electrode (+0.8 mm ML, -5.3 mm AP) and guide cannulae for the working electrode (+0.8 mm ML, +2.0 mm AP) were implanted

and secured with cement along with a silver/silver chloride reference electrode implanted contralateral to the stimulating electrode. Animals were allowed to recover for a minimum of 48 hours before experiments were performed. The stimulating electrode was lowered to 8.5 mm depth to activate the VTA/MFB. The day of experiment, a working electrode was lowered to 7.0 mm depth to measure from the NAc.

Electrodes were fabricated by pulling a 4-barrel microcapillary tube (Stoelting Instrument Co, Chicago, IL) containing a T-650 carbon fiber with a vertical pipette puller (Narishige International USA, East Meadow, NY). The carbon fibers were cut to a length of 50 μm . The resulting probes contained the carbon-fiber electrode, an iontophoresis current return barrel and 2 drug barrels. Electrodes were secured to the animal via a modified Biela manipulator (Crist Instrument Co, Hagerstown, MD). The manipulator was modified to increase the range of motion and provide a means of securing the electrode to the manipulator. The manipulator was attached to a guide cannulae secured to the skull during the surgery. Experiments were performed after at least 2 days recovery from the surgery.

Dopamine concentrations were measured using fast scan cyclic voltammetry (FSCV). The potential waveform used had a -0.4 V holding potential that ramped to 1.3 V and back to -0.4 V at 400 V/s. Waveforms were applied at 5 Hz. The current produced at +0.6 V was used to quantify dopamine concentrations.

Extracellular single unit recordings were collected using SortClient software and analyzed with Neuroexplorer (Plexon Inc, Dallas, TX). The raw data was filtered using a 300 Hz to 3,000 Hz external bandpass filter. Files were collected using the combined voltammetry and physiology system described previously [13].

Intra-cranial self stimulation (ICSS) was performed by providing a 24 pulse, 60 Hz stimulation in the ventral tegmental area (VTA) at 125 μ A in response to the successful press of a lever within an operant chamber. In response to a successful press of the lever, the lever would retract and a tone and houselights would be activated in addition to the stimulation. The tone and houselights would be extinguished 1 second before presentation of the lever. The delay before lever presentation after each press was increased from 1 s to 10 s. Once robust behavior with a 10 s delay was established, 5 -10 sessions consisting of 30 presses each were performed per animal.

RESULTS

The role of D1 receptors in cell activity involved with ICSS behavior was examined. Rats were initially trained to press the lever for the VTA stimulation. Once robust behavior was obtained, the iontophoresis probe was lowered and external unit recordings of spontaneously active cells in the NAc were obtained. The cells showed an inhibition in response to the stimulation (n=3). The iontophoretic ejection of the D1 antagonist, SCH 23390, decreased the baseline firing rate of the neurons (**Figure 4.1**). Once inhibited, the inhibition occurring coincident with the stimulation was no longer observed (**Figure 4.2**).

When introduced by microinjection, SCH 23390 suppresses ICSS behavior [11]. The iontophoretic ejection of SCH 23390 did not affect the behavior, as the ICSS behavior continued throughout the application. The difference is due to the area affected by the injections. Iontophoresis is more localized and therefore only impacts a subsection of the NAc shell while the microinjection affects the entire brain region [14]. This allows

iontophoresis experiments to investigate changes involving dopamine neurotransmission during behavior without risk of modifying the behavior.

The effect of glutamate and dopamine iontophoresis upon spontaneously active cells in the striatum was also investigated. The majority of cells were unable to be affected by either compound's ejection. Of the cells measured ($n = 8$, 7 animals total), only 2 showed an increase in firing rate in response to glutamate ejection. The response of one of the responsive cells to a low (-20 nA) and high (-40 nA) ejection current applied for 30 seconds is shown in **Figure 4.3**. At each of these same 8 cells, a 30 second ejection of dopamine at various currents was applied. A representative trace is shown in **Figure 4.4**. The blue trace is the concentration of ejected dopamine detected at the electrode. These 8 cells, including the two cells responsive to glutamate ejection, failed to display an apparent response to the dopamine ejection.

DISCUSSION

Previous observers have proposed both an inhibitory and excitatory effect of dopamine release [15, 16]. The inhibitory actions are believed to be D2 receptor mediated, while the excitatory actions due to D1 receptor activation [17-20]. By blocking D1 receptors with SCH 23390, an inhibition of tonic firing was obtained as well as removing the phasic response to stimulations during ICSS. The decrease in tonic firing suggests significant D1 receptor occupancy exists throughout the entire recording session in the NAc shell is produces an excitatory effect upon the cell's activity. The loss of the patterned response suggests D1 receptor activation is involved in the response to the stimulation in addition to the tonic activity during ICSS.

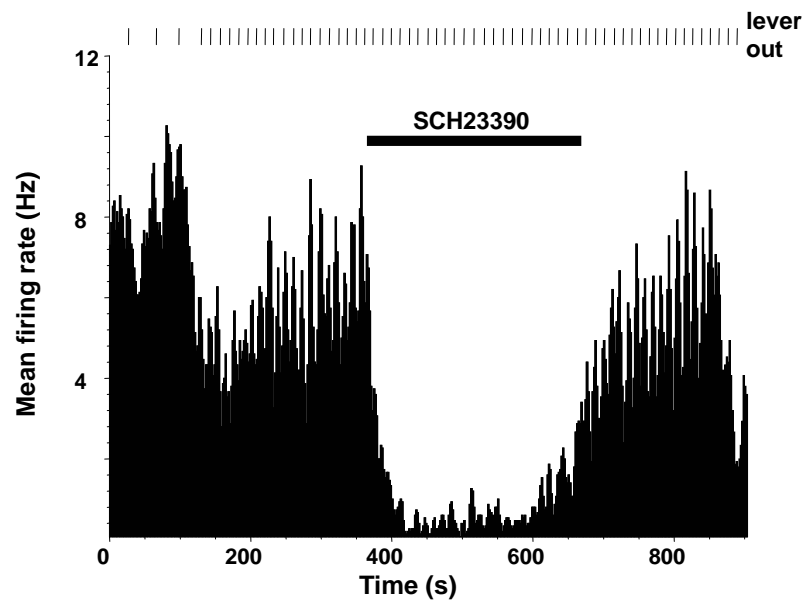


Figure 4.1 D1 dependence of tonic firing. A representative trace showing the decrease in average firing rate of a neuron in the NAc shell in response to 20 nA SCH23390 ejection. The tickmarks along the top show the time of lever press during ICSS. The rate of lever press is unchanged during SCH23390 ejection.

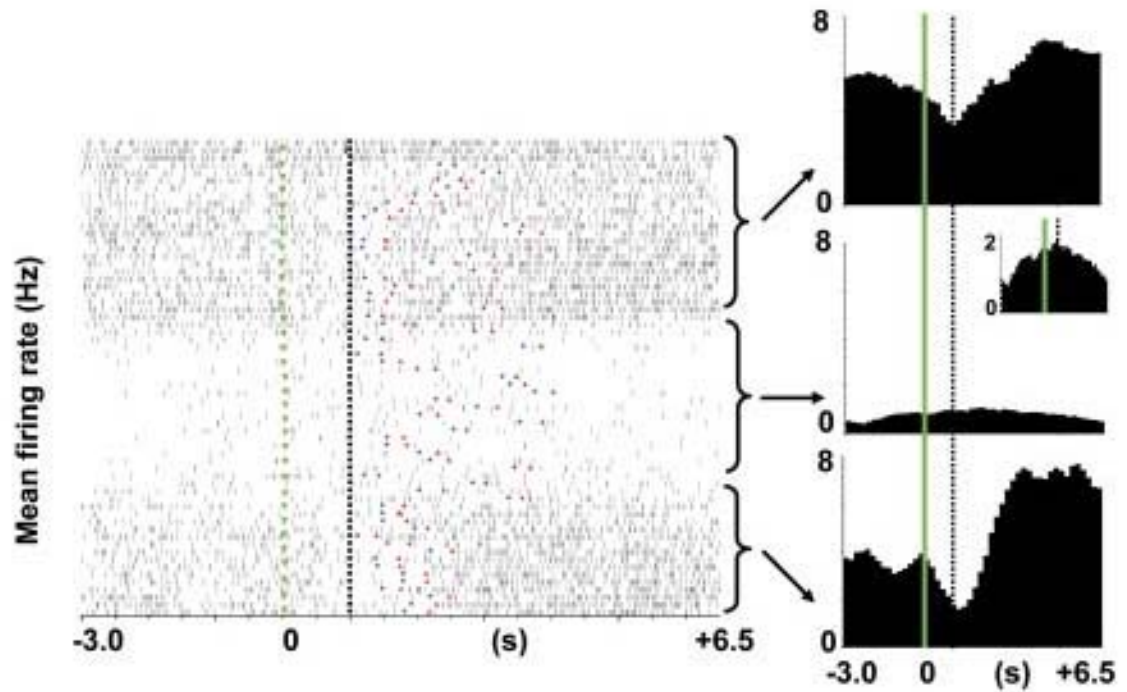


Figure 4.2 D1 affect on patterned firing. The left panel shows each action potential represented as a tick across every trial. The top section is pre-ejection, the middle during 20 nA SCH23390 ejection, and the bottom section post-ejection. The green line shows the presentation of the lever and the black line the lever press. The right panel shows the average firing rate near the lever press for the pre (top), during (middle), and post-ejection (bottom) time periods. The inhibition seen in response to the lever presentation and press is removed during SCH23390 and returns during the post-ejection period.

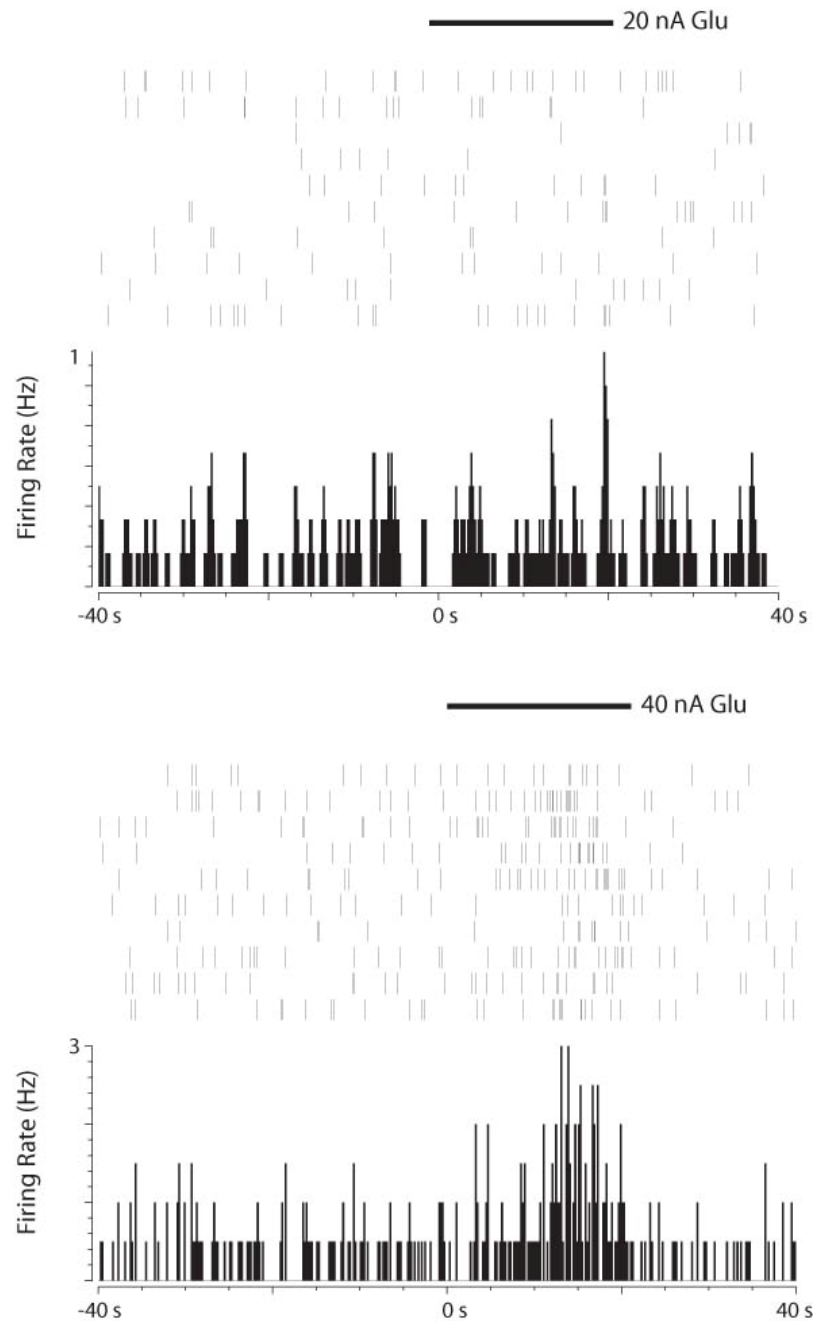


Figure 4.3 Effect of glutamate iontophoresis on spontaneously-active neurons. With relatively large ejection currents (>10 nA) glutamate often failed to elicit a response in the firing rate of spontaneously-active cells in the freely-moving rat striatum. Of the 8 neurons recorded over 7 animals only 2 displayed a response to iontophoretic glutamate ejection, one of which is shown here. The initial -20 nA glutamate ejection (top) failed to generate a response, but an excitation was observed in response to the -40 nA ejection (bottom).

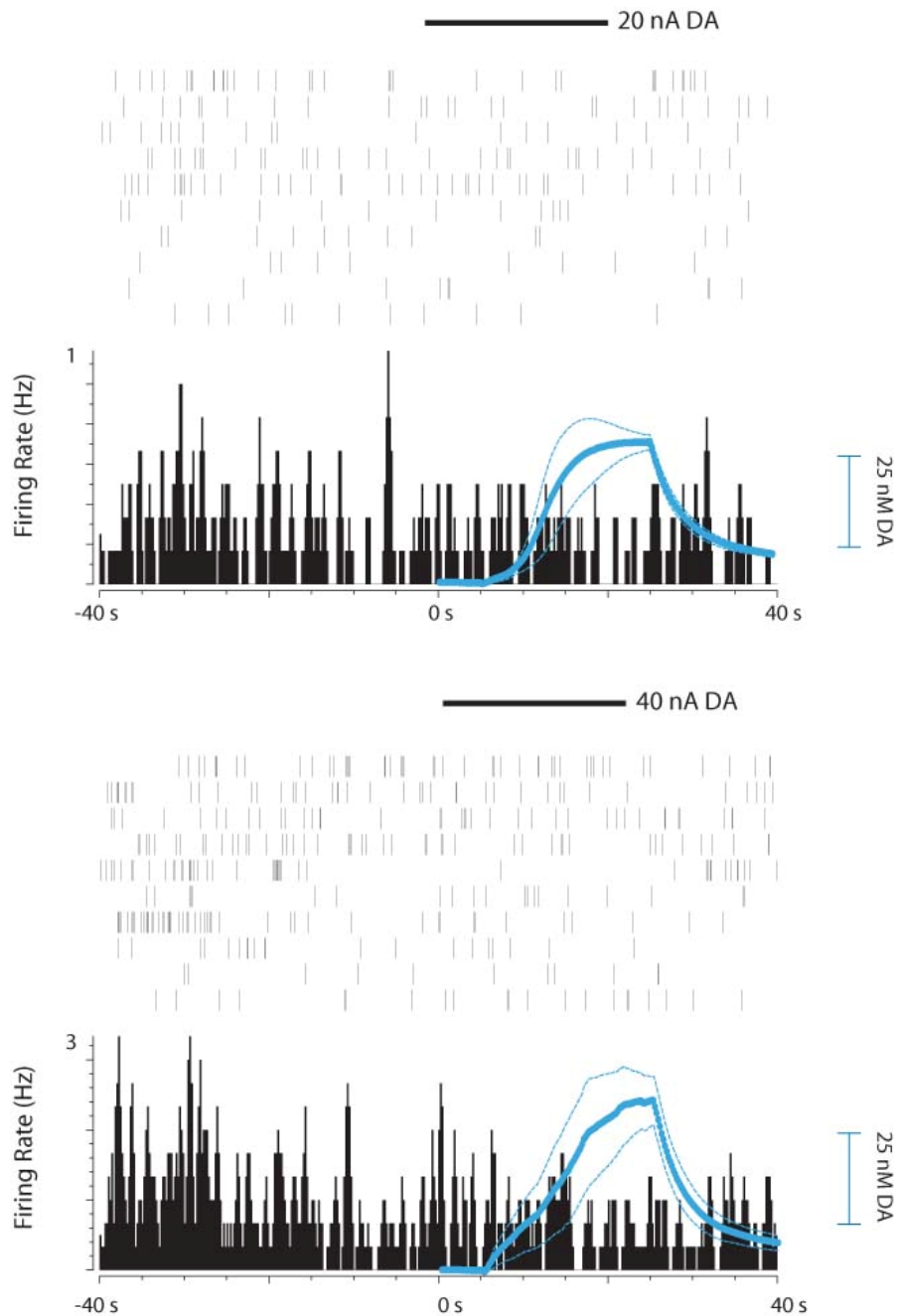


Figure 4.4 Effect of dopamine iontophoresis on spontaneously-active neurons.

Dopamine failed to elicit a response in the firing rate of spontaneously-active cells in the freely-moving rat striatum. Shown is a representative trace of dopamine ejection at +20 nA (top) and +40 nA (bottom) ejection currents. Of the 8 neurons recorded over 7 animals, no neurons displayed a response to iontophoretic dopamine ejection.

The spontaneously-active neurons in the striatum were largely unresponsive to the 20 second ejections of glutamate and dopamine. This finding differs from our results in anesthetized rats. Work by Kiyatkin and coworkers found modest effects by dopamine iontophoresis upon the activity of striatal neurons in freely-moving animals [1]. The same author observed strong responses to glutamate iontophoresis for spontaneously-active cells [21]. A likely reason for the varied results is due to the difference between the sampling of spontaneously active cells versus glutamate-excited cells.

Spontaneously-active cells are detected by slowly lowering the electrode until action potentials sufficiently above the noise-level are obtained. The neuron is estimated to be within approximately 20 μm from the electrode [15]. With the electrode extending 50 μm from the point of iontophoretic ejection, the ejected compound may need to reach a sufficient number of receptors on the dendrites or cell body in sufficient concentrations approximately 70 μm from the point of ejection. For the glutamate-excited neurons in the anesthetized experiments, only those neurons in close proximity to the point of ejection are observed. This is due to the lack of spontaneously active neurons in the striatum of the anesthetized rat. In anesthetized experiments the neurons are required to be responsive to iontophoretic ejection in order to be detected. In the experiment by Kiyatkin and coworkers discussed previously [21], the recording electrode did not extend beyond the point of ejection which would decrease the distance iontophoretic glutamate and dopamine must diffuse in order to reach the target neuron. This difference in electrode construction may explain the contradictory results.

CONCLUSION

The carbon-fiber electrodes combined with iontophoresis were adapted for use in freely-moving animals. The involvement of D1 receptors in tonic and patterned firing of MSNs during ICSS was observed. The ejection of glutamate and dopamine was unable to modify the firing of the majority striatal MSNs. The considerable distance between the point of ejection and the neuron being sampled are likely the cause of the lack of affected cells. These initial experiments show that rapid modification (10-30 s) of neuronal activity will not likely be obtained in the freely-moving animal.

REFERENCES

1. Kiyatkin, E.A. and G.V. Rebec, *Dopaminergic modulation of glutamate-induced excitations of neurons in the neostriatum and nucleus accumbens of awake, unrestrained rats*. J Neurophysiol, 1996. **75**(1): p. 142-53.
2. West, A.R., et al., *Electrophysiological interactions between striatal glutamatergic and dopaminergic systems*. Ann N Y Acad Sci, 2003. **1003**: p. 53-74.
3. Kiyatkin, E.A. and G.V. Rebec, *Modulatory action of dopamine on acetylcholine-responsive striatal and accumbal neurons in awake, unrestrained rats*. Brain Res, 1996. **713**(1-2): p. 70-8.
4. Olds, J. and P. Milner, *Positive reinforcement produced by electrical stimulation of septal area and other regions of rat brain*. J Comp Physiol Psychol, 1954. **47**(6): p. 419-27.
5. Schultz, W., *The Activity of Monkey Midbrain Dopamine Cells in Relation to Initiation and Conduction of Behavioral Acts*. Behavioural Brain Research, 1986. **20**(1): p. 146-146.
6. Garris, P.A., et al., *Real-time measurement of electrically evoked extracellular dopamine in the striatum of freely moving rats*. J Neurochem, 1997. **68**(1): p. 152-61.
7. Rebec, G.V., et al., *Regional and temporal differences in real-time dopamine efflux in the nucleus accumbens during free-choice novelty*. Brain Res, 1997. **776**(1-2): p. 61-7.
8. Robinson, D.L., M.L. Heien, and R.M. Wightman, *Frequency of dopamine concentration transients increases in dorsal and ventral striatum of male rats during introduction of conspecifics*. J Neurosci, 2002. **22**(23): p. 10477-86.
9. Roitman, M.F., et al., *Dopamine operates as a subsecond modulator of food seeking*. Journal of Neuroscience, 2004. **24**(6): p. 1265-1271.
10. Stuber, G.D., et al., *Rapid dopamine signaling in the nucleus accumbens during contingent and noncontingent cocaine administration*. Neuropsychopharmacology, 2005. **30**(5): p. 853-863.
11. Cheer, J.F., et al., *Coordinated accumbal dopamine release and neural activity drive goal-directed behavior*. Neuron, 2007. **54**(2): p. 237-244.
12. Armstrong-James, M., J. Millar, and Z.L. Kruk, *Quantification of noradrenaline iontophoresis*. Nature, 1980. **288**(5787): p. 181-3.

13. Cheer, J.F., et al., *Simultaneous dopamine and single-unit recordings reveal accumbens GABAergic responses: implications for intracranial self-stimulation*. Proc Natl Acad Sci U S A, 2005. **102**(52): p. 19150-5.
14. Hicks, T.P., *The history and development of microiontophoresis in experimental neurobiology*. Prog Neurobiol, 1984. **22**(3): p. 185-240.
15. Williams, G.V. and J. Millar, *Concentration-dependent actions of stimulated dopamine release on neuronal activity in rat striatum*. Neuroscience, 1990. **39**(1): p. 1-16.
16. Hu, X.T. and F.J. White, *Dopamine enhances glutamate-induced excitation of rat striatal neurons by cooperative activation of D1 and D2 class receptors*. Neurosci Lett, 1997. **224**(1): p. 61-5.
17. Cepeda, C., N.A. Buchwald, and M.S. Levine, *Neuromodulatory actions of dopamine in the neostriatum are dependent upon the excitatory amino acid receptor subtypes activated*. Proc Natl Acad Sci U S A, 1993. **90**(20): p. 9576-80.
18. Surmeier, D.J., et al., *Modulation of calcium currents by a D1 dopaminergic protein kinase/phosphatase cascade in rat neostriatal neurons*. Neuron, 1995. **14**(2): p. 385-97.
19. Hernandez-Lopez, S., et al., *D2 dopamine receptors in striatal medium spiny neurons reduce L-type Ca²⁺ currents and excitability via a novel PLC[β]/IP₃-calcineurin-signaling cascade*. J Neurosci, 2000. **20**(24): p. 8987-95.
20. West, A.R. and A.A. Grace, *Opposite influences of endogenous dopamine D1 and D2 receptor activation on activity states and electrophysiological properties of striatal neurons: studies combining in vivo intracellular recordings and reverse microdialysis*. J Neurosci, 2002. **22**(1): p. 294-304.
21. Kiyatkin, E.A. and G.V. Rebec, *Modulation of striatal neuronal activity by glutamate and GABA: iontophoresis in awake, unrestrained rats*. Brain Res, 1999. **822**(1-2): p. 88-106.

CHAPTER 5

ESTIMATING THE BASAL DOPAMINE LEVEL WITH FAST SCAN CYCLIC VOLTAMMETRY

INTRODUCTION

The “basal dopamine level” refers to the average dopamine concentration observed throughout the extracellular fluid within a given brain region. This dopamine level, while not tracking individual release events, is sensitive to behavioral events and drug administration. The basal dopamine concentration is of substantial importance since changes in the dopamine basal level would impact overall signal processing within the NAc.

The magnitude of the basal level is regulated by the balance between dopamine release and clearance. Uptake via the dopamine transporter (DAT) is the predominant method in which dopamine is cleared from the extracellular space in the striatum and NAc. In order to generate a persistent dopamine concentration, dopamine release must reach an equilibrium level with or exceed DAT function. The characteristics of the release events, including the magnitude and frequency as well as the number of release sites, will determine the basal concentration [1].

Vesicular release is commonly considered the primary source of extracellular dopamine. Released in response to action potentials, the amount of dopamine released is dependent upon the number and frequency of action potentials the cell exhibits. Dopamine neurons display two modes of firing, phasic and non-phasic firing. Non-phasic firing describes the generation of action potentials at a consistent 3-7 Hz and is the predominant mode [2, 3]. The phasic mode consists of short, intermittent bursts consisting of several action potentials at ~20 Hz [4, 5]. Models of extracellular dopamine concentrations arising from vesicular release predict that low frequency release events reach an equilibrium level

with uptake while extracellular dopamine from high frequency events saturates the DAT, continually increasing dopamine levels over the duration of the event [1, 6]. The predicted concentrations profiles corresponded well with electrochemical recordings at a range of stimulation frequencies.

Action potential-dependent vesicular release is not the only potential source, however. During amphetamine administration, it was discovered that the dopamine transporter can reverse its action and extrude dopamine from the neuron into the extracellular space [7, 8]. This process, known as reverse transport, provides a non-vesicular method of increasing extracellular dopamine that is also independent of neuronal firing rate. Reverse transport is believed to occur rarely under normal physiological conditions [9]. However, recent publications have proposed that the process may occur during normal neural activity in the absence of amphetamine at sufficient rates to impact basal dopamine levels [10]. In order to estimate the basal dopamine level, the change in dopamine concentration detected with FSCV was measured while potential sources of extracellular dopamine were blocked pharmacologically.

METHODS

Male Sprague-Dawley rats were anesthetized and surgery performed as described previously for freely moving experiments. The stimulating electrode contained a guide cannula for a microinjection needle located between the prongs of the stimulator. This ensured the region affected by the microinjection was identical to the region being stimulated. The day of experiment a carbon fiber electrode was lowered to the NAc and maximal dopamine release from a 24 pulse, 125 μ A stimulation train was obtained. Fifteen

minutes of background data was collected to ensure a stable background with minimal drift was present. After a stable signal was obtained, 500 nL of saline solution was injected and changes in dopamine concentration were measured for 15 minutes. This experiment served as a control for the subsequent experiment in which 500 ng of lidocaine was injected and dopamine was measured for 15 minutes. Stimulation trains were applied before and after each 15 minute session. A second series of experiments consisted of lidocaine microinjection followed by i.v. administration of cocaine (1 mg/kg in saline) through an implanted jugular vein catheter and measuring dopamine for 10 minutes post-infusion.

Data analysis was performed using principle component regression software [11]. Training sets for dopamine and pH were constructed for each experiment using various concentrations collected by manipulating the stimulation train pulse number or frequency. All electrodes were calibrated in vitro using a range of dopamine concentrations between 100 nM to 1 μ M and a single-point pH calibration.

Averaged dopamine traces were analyzed for significance using a bin by bin Z test with 10 second bins. Concentrations were considered not significant if below the requirements for 99% confidence. All error bars represent the SEM of the averaged concentration traces.

RESULTS

The results from a single animal measured during electrical stimulation and saline infusion into the VTA/SN are shown in **Figure 5.1**. In this animal, electrical stimulation evoked a 65 nM dopamine concentration change. The pH trace indicates a transient acidic shift during the stimulation that is followed by a 0.18 pH units basic shift after the

stimulation. Next, saline (500 nL) was infused into the VTA/SN for 1 min. Changes in dopamine and pH extracted by principle component analysis during the infusion interval were smaller than during the stimulation with fluctuations less than 30 nM detected. The voltammetric results obtained during the minute after infusion are shown as a continuation of these recordings and similarly show very small changes in dopamine and pH. The electrical stimulation after this two minute interval is quite similar to that before the saline infusion. This experiment was repeated in five animals and the average dopamine responses during the infusion minute and the subsequent minute are shown in **Figure 5.2**. The dopamine changes are not significant.

Figure 5.2 shows data from the same animal shown in **Figure 5.1**. The experiment is identical except lidocaine is infused instead of saline. The first electrical stimulation evokes pH and dopamine changes as before. During the lidocaine infusion (500 nL containing 500 ng over 1 min) smaller changes in dopamine less than 30 nM and pH are seen than during the electrical stimulation. During the electrical stimulation after the lidocaine the responses to both pH and dopamine are dramatically suppressed to 20 nM and .05 pH units respectively. This experiment was repeated in 5 animals and the mean concentration of dopamine during and following lidocaine infusion is also shown in **Figure 5.3**. There was no significant dopamine change.

I.V. administration of cocaine causes a large increase in extracellular dopamine concentration in the NAc that persists for a few minutes [12]. In this work, cocaine (3 mg/kg, i.v.) was administered following saline infusion into the VTA/SN and similar increases were obtained (n =5). This cocaine-induced increase in extracellular dopamine was

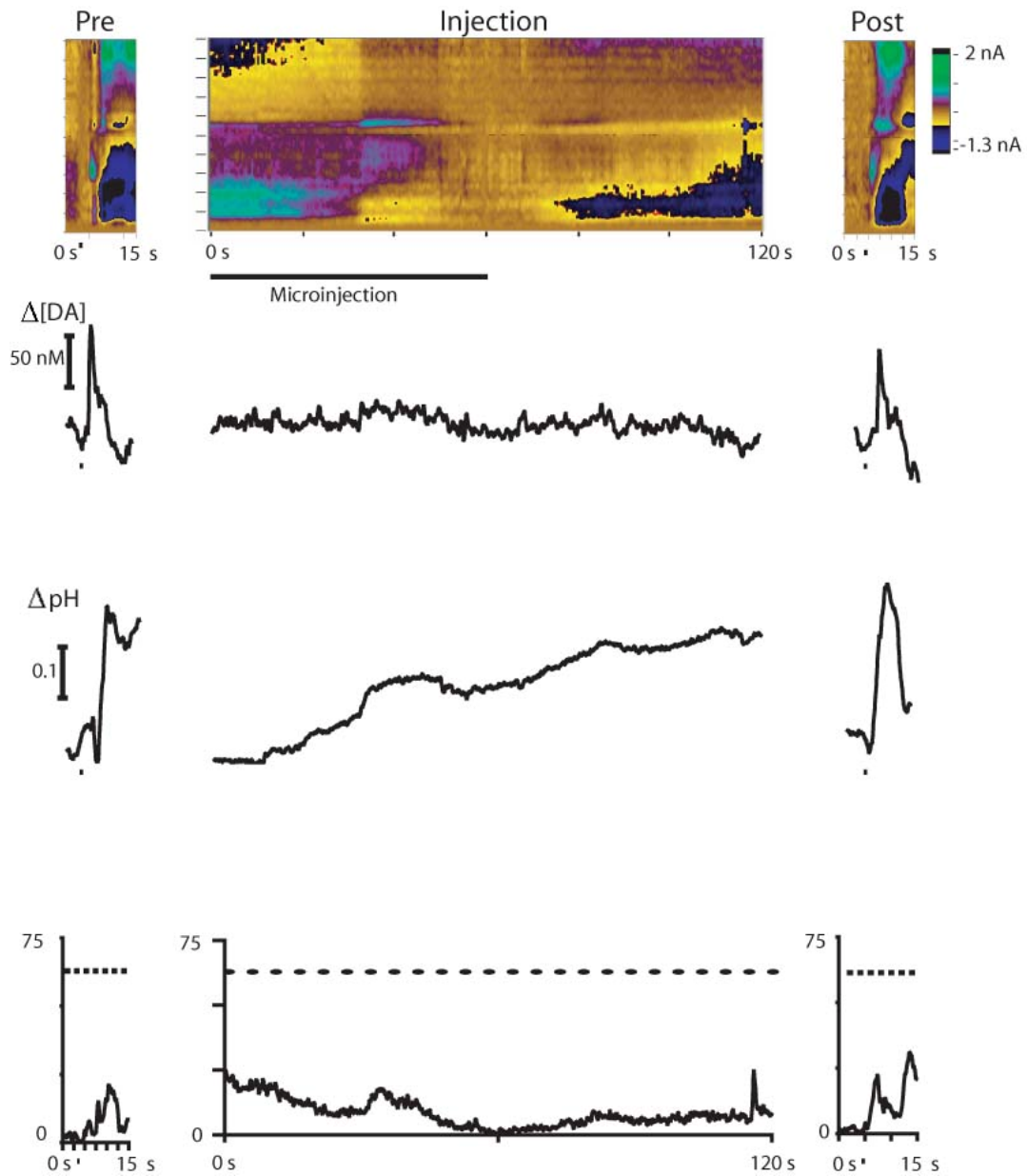


Figure 5.1: Saline microinjection. The left panel shows the pre-injection stimulated release data for a single trial. The color plots obtained from a representative animal are shown for the pre-infusion stimulation (left), 500 nL saline infusion (middle), and post-infusion stimulation (right). Below the color plots are the changes in dopamine concentration (top trace) and changes in pH (middle trace) obtained through PCR analysis of the data displayed in the color plot. The Q-value (bottom trace) generated by the PCR analysis is shown.

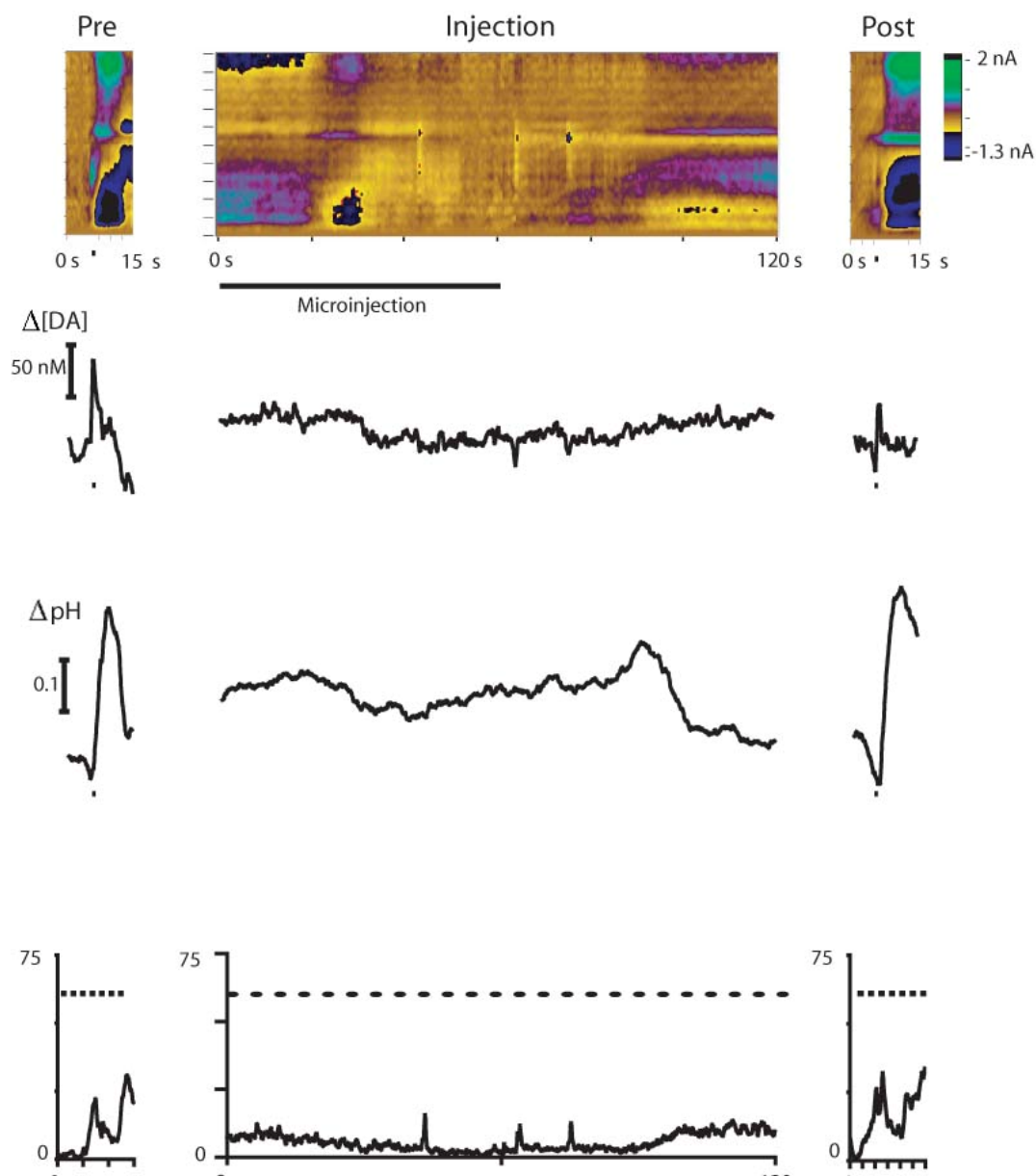
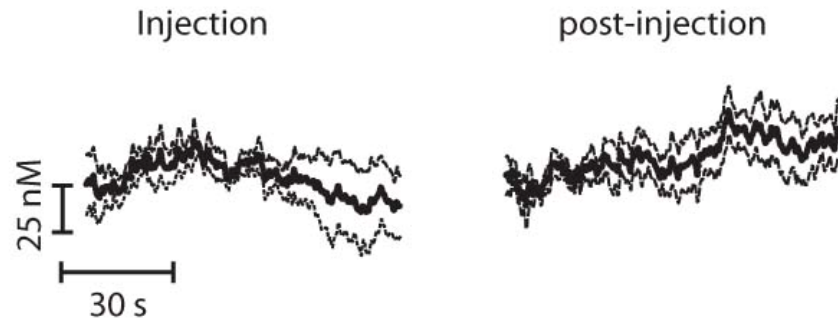


Figure 5.2: Lidocaine microinjection. The left panel shows the pre-injection stimulated release data for a single trial. The color plots obtained from a representative animal are shown for the pre-infusion stimulation (left), 500 ng lidocaine infusion (middle), and post-infusion stimulation (right). Below the color plots are the changes in dopamine concentration (top trace) and changes in pH (middle trace) obtained through PCR analysis of the data displayed in the color plot. The Q-value (bottom trace) generated by the PCR analysis is shown.

A. Saline



B. Lidocaine

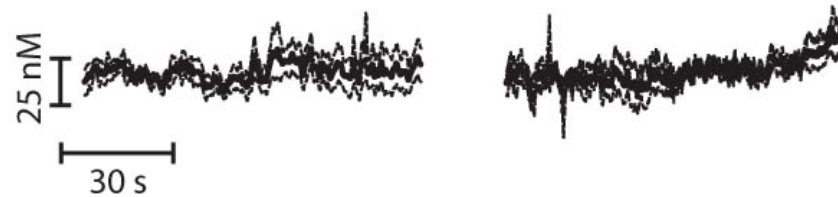


Figure 5.3: Average dopamine response to saline and lidocaine microinjection. **A.** The average DA concentration changes during (left) and following (right) microinjection of 500 nL saline into the VTA ($n=5$). The fluctuations in dopamine concentration were not significant ($p < .01$). **B.** The average DA concentration changes during (left) and following (right) microinjection of lidocaine (500 nL of solution containing 500 ng lidocaine) into the VTA ($n=5$). The fluctuations in dopamine concentration were not significant ($p < .01$). The dashed lines represent the SEM of the concentrations.

dramatically diminished in animals that receive VTA/SN injections of lidocaine (500 ng, n = 5) and the average normalized changes in dopamine levels are shown in **Figure 5.4**.

DISCUSSION

Blocking sources of extracellular dopamine

Microinjection of the sodium channel blocker, lidocaine, into the VTA reduced impulse-dependent dopamine release as evidenced by the decrease in stimulated dopamine release. Lidocaine injection in the primate cerebral cortex showed a 60% decrease in neuronal firing rates within one minute after infusion [13]. Injection into the VTA has been shown to significantly decrease basal dopamine levels according to microdialysis measurements in the NAc [14]. The reduction in impulse-dependant dopamine release failed to generate a detectable decrease in basal dopamine concentration.

The hypothesis that reverse transport of dopamine generates a large basal concentration predicts that cocaine administration will produce a significant dopamine decrease. However, cocaine substantially increases dopamine levels as seen in **Figure 5.4** and in previous studies [12]. The increase could be due to enhanced transient dopamine release and not indicative of basal levels however, thereby compensating for a decrease generated from blocking reverse transport. Therefore lidocaine was administered prior to cocaine infusion. With both impulse-dependent release and reverse transport blocked, the dopamine basal level should be drastically altered. The combination of both drugs did not produce a reduction in dopamine levels. A slight increase in dopamine was obtained instead.

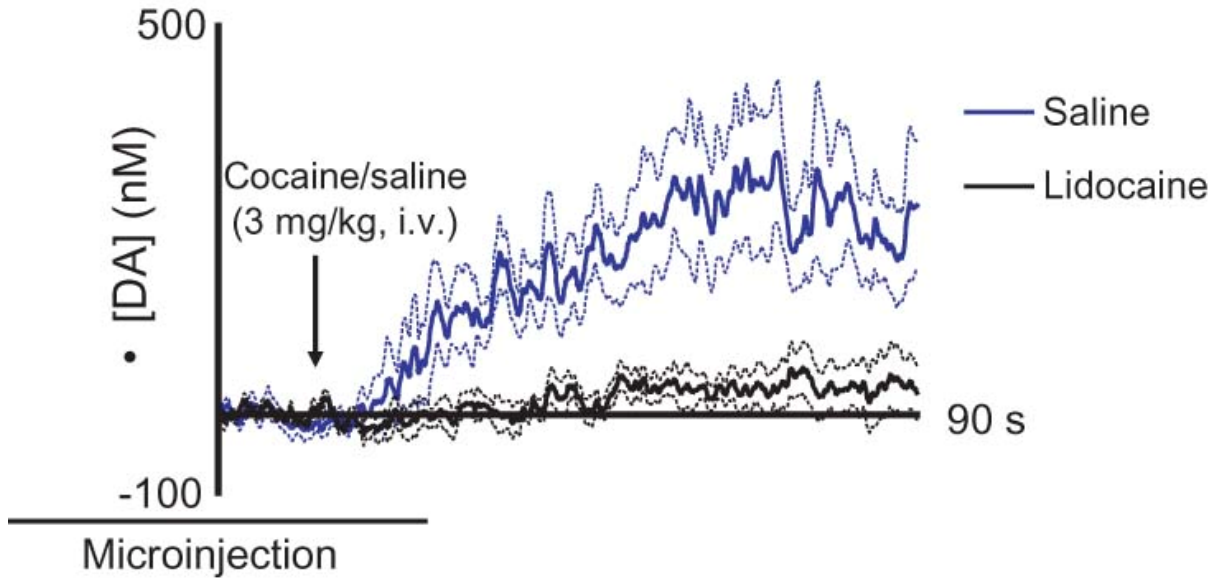


Figure 5.4: Cocaine and lidocaine injection. The blue trace displays the average dopamine concentration with saline microinjection followed by i.v. cocaine administration ($n=5$). The black trace is the average dopamine concentration with lidocaine microinjection followed by cocaine administration ($n=5$). The dashed lines represent the SEM of the averaged concentrations. The 50 second duration of the infusion of saline or lidocaine is shown by the dark line below the figure. Infusions were initiated 20 seconds before data collection and the lasted for the first 30 seconds of data collection. Cocaine (3 mg/kg, i.v.) was injected after 20 seconds of data collection.

Previous basal level estimates

Multiple techniques have been employed to measure basal dopamine levels. Binding assays with radio-labeled dopamine estimated basal dopamine levels of 60-100 nM [15, 16]. The measurements are not direct however, and are based upon estimates of average receptor occupancy. Capable of directly measuring low nanomolar concentrations with exceptional chemical selectivity in vivo, microdialysis emerged as the technique of choice for measuring basal dopamine concentrations. The simplest treatment of microdialysis data follows the equation [17]:

$$C_{in\ vivo} = \left(\frac{K\lambda^2}{\alpha} \right) \left(\frac{C_{dial}}{Rec_{in\ vitro}} \right)$$

$C_{in\ vivo}$ is the concentration in the brain, C_{dial} is the concentration measured by microdialysis, and α and λ account for the volume fraction and tortuosity of the tissue, respectively. The concentration of analyte detected in the dialysate does not equal the concentration in bulk solution, so a recovery factor is required to correlate the concentration outside the probe to the concentration in the dialysate. The factor, $Rec_{in\ vitro}$, is the recovery factor in buffer containing a known analyte concentration. The empirically-derived value, K , represents a correction factor to account for the difference between the in vivo and in vitro recovery factor. Unless actual in vivo concentrations are known, K is impossible to obtain and ignored in early experiments. These experiments measured the values of dopamine in the dialysate and applied the extraction factor generated with in vitro calibrations. These studies reported a 1-2 μ M basal dopamine level [17, 18]. The reported values were later believed to

be grossly overestimated as evidence emerged suggesting the extraction factor was significantly altered in vivo [19]. Recent advances allowing lower flow rates produced an estimated basal level of 25 nM using an in vitro recovery factor [20].

In an effort to circumvent the inability to accurately determine the extraction factor in vivo, microdialysis studies were reworked using no-net flux dialysis [21]. In no-net flux, incremental amounts of analyte are introduced to the dialysate. When dialysate levels are lower than the in vivo concentrations, analyte molecules diffuse into the probe and an increase in analyte level is detected. Likewise, when dialysate levels are higher than found in vivo, analyte diffuses out of the probe and detected levels decrease. Graphing this data determines the zero point at which no net flux exists. This point of no net flux is believed to be the actual concentration of analyte in vivo. No-net flux dialysis obtained a low nanomolar basal dopamine level [22]. The technique is not perfect, however, since it assumes the efficiency analyte efflux from the probe is identical to the influx from the tissue [23].

A second solution to this problem is variable flow microdialysis. The recovery rate is inversely proportional to the rate of dialysate flow rate within the probe, therefore when the flow rate is zero, the recovery rate is infinite and therefore dialysate and in vivo concentrations are equal. By measuring the analyte signal at multiple flow rates, a curve is produced which allows calculation of the concentration of analyte at zero flow [24]. The two microdialysis techniques were directly compared and delivered similar results [19].

Of importance is that the dimensions of microdialysis probes are sufficient to generate significant damage to the tissue [25, 26]. The damage layer was found to have minimal dopamine release but uptake remained active which may cause the concentrations near the probe to differ from the concentration in healthy tissue. The damage layer therefore

may cause dialysis measurements to underestimate basal levels [27]. The damaged tissue can be corrected for to improve the accuracy of measurements, though a more detailed model of the damage layer needs to be developed to improve the correction factors [28].

Electrochemistry at carbon-fiber electrodes has been employed to measure basal concentrations previously. Differential pulse voltammetry was applied to estimate the basal levels of several catecholamines and ascorbic acid in the striatum and detected a 26 nM basal dopamine level [29]. A recent study employed FSCV to estimate basal dopamine levels and obtained a 2 μ M concentration [10]. In the study, a non-specific glutamate receptor antagonist, kynurenate, was administered and cyclic voltammograms recorded for over 30 minutes. Background subtractions were performed across the entire recording period and a dopaminergic decrease was detected. The large charging current generated in FSCV is stable over short time periods of 90 seconds or less, so background subtraction is used in order to accurately detect and quantify dopamine release. Considerable drift in the charging current will occur over the course of the experiment, and was corrected for with a factor calculated through comparison of currents generated at voltages at which dopamine is not oxidized or reduced. The experimenters proposed the hypothesis that the large basal level is maintained through glutamate-dependant reverse transport through the dopamine transporter.

Using rapid concentration changes to estimate basal levels

The timescale of the lidocaine and cocaine with lidocaine experiments are substantially shorter than used in the kynurenate study. However, robust effects were witnessed within the initial moments after kynurenate infusion in that experiment [30]. Changes in uptake rate on the same timescale as transient dopamine release events are also

hypothesized by the authors to lead to substantial decreases in basal concentrations [31]. Therefore, blockade of both impulse-dependent and independent sources of extracellular dopamine levels should produce significant changes in the basal dopamine level within the time constraints imposed in this study.

A decrease in a large, micromolar-scale basal level would have been readily detected with FSCV. Instead, only a modest decrease in dopamine concentration not significantly different from saline control was detected. Estimates for FSCV sensitivity are near 10 nM [32]. The basal dopamine levels from no-net flux and recent microdialysis experiments estimate a basal level near or below the detection limit for FSCV. The lack of significant shift in dopamine is therefore consistent with the microdialysis estimates.

CONCLUSION

Uncertainty exists in all FSCV studies as to what level of dopamine exists in addition to the detected transient dopamine release. In order to correlate FSCV results to microdialysis measurements or assign behavioral significance to transient dopamine signals, the concentration of basal dopamine must be known. The variability within literature values of basal dopamine levels led to an investigation using FSCV. Direct measurement of tonic concentrations is not possible, so the strategy was to pharmacologically block sources of extracellular dopamine and monitor any resulting decreases in dopamine. The experiment required rapid cessation of impulse-dependent dopamine release and blocking reverse transport. With the nullification of the two main potential sources for extracellular dopamine, the presence of a large, micromolar basal dopamine concentration should become evident through a decrease in dopamine levels. Blocking reverse transport was achieved by

administration of cocaine which inhibits the dopamine transporter. Though unable to produce a direct measure of the basal level, the investigation was capable of providing evidence supporting a low nanomolar basal concentration.

REFERENCES

1. Venton, B.J., et al., *Real-time decoding of dopamine concentration changes in the caudate-putamen during tonic and phasic firing*. J Neurochem, 2003. **87**(5): p. 1284-95.
2. Grace, A.A. and B.S. Bunney, *The Control of Firing Pattern in Nigral Dopamine Neurons - Single Spike Firing*. Journal of Neuroscience, 1984. **4**(11): p. 2866-2876.
3. Schultz, W., *The Activity of Monkey Midbrain Dopamine Cells in Relation to Initiation and Conduction of Behavioral Acts*. Behavioural Brain Research, 1986. **20**(1): p. 146-146.
4. Grace, A.A., *The Tonic Phasic Model of Dopamine System Regulation - Its Relevance for Understanding How Stimulant Abuse Can Alter Basal Ganglia Function*. Drug and Alcohol Dependence, 1995. **37**(2): p. 111-129.
5. Hyland, B.I., et al., *Firing modes of midbrain dopamine cells in the freely moving rat*. Neuroscience, 2002. **114**(2): p. 475-492.
6. Wightman, R.M. and J.B. Zimmerman, *Control of dopamine extracellular concentration in rat striatum by impulse flow and uptake*. Brain Res Brain Res Rev, 1990. **15**(2): p. 135-44.
7. Raiteri, M., et al., *Dopamine Can Be Released by 2 Mechanisms Differentially Affected by the Dopamine Transport Inhibitor Nomifensine*. Journal of Pharmacology and Experimental Therapeutics, 1979. **208**(2): p. 195-202.
8. Fischer, J.F. and A.K. Cho, *Chemical release of dopamine from striatal homogenates: evidence for an exchange diffusion model*. J Pharmacol Exp Ther, 1979. **208**(2): p. 203-9.
9. Jones, S.R., et al., *Dopamine neuronal transport kinetics and effects of amphetamine*. J Neurochem, 1999. **73**(6): p. 2406-14.
10. Borland, L.M. and A.C. Michael, *Voltammetric study of the control of striatal dopamine release by glutamate*. J Neurochem, 2004. **91**(1): p. 220-9.
11. Heien, M.L., M.A. Johnson, and R.M. Wightman, *Resolving neurotransmitters detected by fast-scan cyclic voltammetry*. Anal Chem, 2004. **76**(19): p. 5697-704.
12. Heien, M.L., et al., *Real-time measurement of dopamine fluctuations after cocaine in the brain of behaving rats*. Proc Natl Acad Sci U S A, 2005. **102**(29): p. 10023-8.

13. Tehovnik, E.J. and M.A. Sommer, *Effective spread and timecourse of neural inactivation caused by lidocaine injection in monkey cerebral cortex*. J Neurosci Methods, 1997. **74**(1): p. 17-26.
14. Howland, J.G., P. Taepavarapruk, and A.G. Phillips, *Glutamate receptor-dependent modulation of dopamine efflux in the nucleus accumbens by basolateral, but not central, nucleus of the amygdala in rats*. J Neurosci, 2002. **22**(3): p. 1137-45.
15. Ross, S.B., *Synaptic concentration of dopamine in the mouse striatum in relationship to the kinetic properties of the dopamine receptors and uptake mechanism*. J Neurochem, 1991. **56**(1): p. 22-9.
16. Delforge, J., et al., *Absolute quantification by positron emission tomography of the endogenous ligand*. J Cereb Blood Flow Metab, 2001. **21**(5): p. 613-30.
17. Benveniste, H. and P.C. Huttemeier, *Microdialysis--theory and application*. Prog Neurobiol, 1990. **35**(3): p. 195-215.
18. Lindefors, N., G. Amberg, and U. Ungerstedt, *Intracerebral microdialysis: I. Experimental studies of diffusion kinetics*. J Pharmacol Methods, 1989. **22**(3): p. 141-56.
19. Parsons, L.H. and J.B. Justice, Jr., *Extracellular concentration and in vivo recovery of dopamine in the nucleus accumbens using microdialysis*. J Neurochem, 1992. **58**(1): p. 212-8.
20. Shou, M., et al., *Monitoring dopamine in vivo by microdialysis sampling and on-line CE-laser-induced fluorescence*. Anal Chem, 2006. **78**(19): p. 6717-25.
21. Lonnroth, P., P.A. Jansson, and U. Smith, *A microdialysis method allowing characterization of intercellular water space in humans*. Am J Physiol, 1987. **253**(2 Pt 1): p. E228-31.
22. Sam, P.M. and J.B. Justice, Jr., *Effect of general microdialysis-induced depletion on extracellular dopamine*. Anal Chem, 1996. **68**(5): p. 724-8.
23. Peters, J.L. and A.C. Michael, *Modeling voltammetry and microdialysis of striatal extracellular dopamine: the impact of dopamine uptake on extraction and recovery ratios*. J Neurochem, 1998. **70**(2): p. 594-603.
24. Jacobson, I., M. Sandberg, and A. Hamberger, *Mass transfer in brain dialysis devices--a new method for the estimation of extracellular amino acids concentration*. J Neurosci Methods, 1985. **15**(3): p. 263-8.

25. Benveniste, H. and N.H. Diemer, *Cellular Reactions to Implantation of a Microdialysis Tube in the Rat Hippocampus*. Acta Neuropathologica, 1987. **74**(3): p. 234-238.
26. Damsma, G., et al., *Analysis and Microdialysis of Acetylcholine in the Brain of Freely Moving Rats*. Pharmaceutisch Weekblad-Scientific Edition, 1987. **9**(6): p. 338-338.
27. Borland, L.M., et al., *Voltammetric study of extracellular dopamine near microdialysis probes acutely implanted in the striatum of the anesthetized rat*. J Neurosci Methods, 2005. **146**(2): p. 149-58.
28. Bungay, P.M., et al., *Microdialysis of dopamine interpreted with quantitative model incorporating probe implantation trauma*. J Neurochem, 2003. **86**(4): p. 932-46.
29. Gonon, F.G. and M.J. Buda, *Regulation of Dopamine Release by Impulse Flow and by Autoreceptors as Studied by Invivo Voltammetry in the Rat Striatum*. Neuroscience, 1985. **14**(3): p. 765-774.
30. Kulagina, N.V., M.J. Zigmond, and A.C. Michael, *Glutamate regulates the spontaneous and evoked release of dopamine in the rat striatum*. Neuroscience, 2001. **102**(1): p. 121-8.
31. Michael, A.C., et al., *Theory for the impact of basal turnover on dopamine clearance kinetics in the rat striatum after medial forebrain bundle stimulation and pressure ejection*. J Neurochem, 2005. **94**(5): p. 1202-11.
32. Heien, M.L., et al., *Overoxidation of carbon-fiber microelectrodes enhances dopamine adsorption and increases sensitivity*. Analyst, 2003. **128**(12): p. 1413-9.

CHAPTER 6

COCAINE INCREASES DOPAMINE RELEASE BY MOBALIZATION OF A SYNAPSIN-DEPENDENT RESERVE POOL

INTRODUCTION

Dopamine neurons in the midbrain are synchronously and transiently activated by presentation of salient stimuli, including those that predict reinforcers [1]. These neurons project to areas of the forebrain that ultimately modulate motor performance. Indeed, striatal dopaminergic terminals are strategically located to play a central role in sensorimotor integration [2]. Recent findings demonstrate that transient dopamine surges occur in the striatum in response to important natural [3] or drug-related stimuli [4], and that these transients are involved in directing the animal's behavior. Cocaine, an important drug of abuse, enhances sensorimotor reactivity through its action on dopamine terminals [5]. Indeed, physiological and emotional responses to drug-related sensory stimuli are enhanced following cocaine use in humans [6].

The mechanisms through which cocaine enhances dopaminergic neurotransmission have long been debated [7]. It is well established that cocaine competitively inhibits the dopamine transporter (DAT), thereby elevating extracellular levels of dopamine [8]. However, several reports point toward the possibility that cocaine and other psychostimulants can also affect *release* of dopamine [9, 10]. The first indication of an effect of cocaine on dopamine release came from the observation that cocaine and other non-amphetamine psychostimulants can still stimulate the CNS even after dopamine availability is limited by inhibiting its synthesis [11]. These results were interpreted to mean that the psychostimulants act by mobilizing a storage pool of dopamine. Support for this interpretation was provided by the demonstration that one of these psychostimulants,

amfonelic acid, can restore dopamine release following depletion of newly synthesized dopamine with α -methyl-*p*-tyrosine (α MPT;[12]). While these findings were intriguing, they were unable to elucidate cellular or molecular substrates for this postulated cocaine-sensitive storage pool.

More recent studies of other neurotransmitter systems have shown that several different pools of secretory vesicles exist (reviewed in [13]). These include a releasable pool of vesicles that are available for immediate exocytosis and a reserve pool of vesicles that are spatially segregated and mobilized following prolonged synaptic activity [14-18]. Thus, it is possible that cocaine could also mobilize dopaminergic vesicles from such a reserve pool. Here we consider this hypothesis by using mice in which all three known synapsin genes have been disrupted, synapsin I/II/ III triple-knockout (TKO) mice. Synapsins are phosphoproteins that interact with the surface of synaptic vesicles and segregate synaptic vesicles into the reserve pool[19, 20]. These mice are viable but have severe deficits in their synaptic vesicle reserve pools [21]. We find that cocaine enhances dopamine released by stimuli that mobilize vesicles from the reserve pool in wild-type mice but has little effect on dopamine release in the TKO mice. These results indicate that cocaine enhances dopamine release by mobilizing a synapsin-dependent reserve pool of dopamine-containing synaptic vesicles.

METHODS

Surgery

Synapsin (I/II/III) TKO and wild type (WT) mice were generated at The Rockefeller University and bred at Duke University, as described elsewhere [21, 22]. Animals were

anesthetized with urethane (1.5 g/kg i.p.) and placed in a stereotaxic frame. The coordinates for placement of the working-electrode in the caudate-putamen are (in mm from bregma): AP +1.1, ML +1.2 and DV -2.2. The stimulating electrode was placed in the medial forebrain bundle at AP -2.4, ML +1.1, DV -4.5. The dorsal-ventral placement of both the working and stimulating electrodes was adjusted in small increments to find maximal dopamine release. An Ag/AgCl reference electrode was inserted into the contralateral side of the brain.

Electrochemistry

Dopamine was detected with 50 μm long cylindrical carbon-fiber microelectrodes [23]. Dopamine signals were identified with fast-scan cyclic voltammetry with a voltage scan from -0.4 V to 1.0 V and back at 300 V/s, repeated every 100 ms. For pharmacology experiments, once a dopamine release site was identified with cyclic voltammetry, constant-potential amperometry (+0.3 V) was used because it has a more rapid time response [23]. Electrodes were calibrated *in vitro* after the experiment using known concentrations of dopamine.

Data analysis

Amperometric data recorded during 24 pulse stimulations were modeled [24] by assuming that each stimulus pulse evokes an increase in the extracellular concentration of dopamine ($[\text{DA}]_p$). In the time between stimulus pulses and after the stimulus train, uptake of dopamine by the DAT was assumed to follow Michaelis-Menten kinetics with an apparent affinity for dopamine (K_m) of 0.2 μM in WT mice [24, 25] and a maximum rate of uptake of the DAT (V_{max}) that is a function of the density of proximal uptake sites. The simulation also

included an apparent distance (d_{app}) that dopamine can diffuse. After block of uptake by competitive inhibitors, V_{max} was kept constant and the remaining parameters were allowed to vary until optimal fit to the data was obtained. Statistical comparisons were performed in Microsoft Excel using t-tests. Data are reported as mean \pm SEM and were considered significant at $p < 0.05$.

Drugs

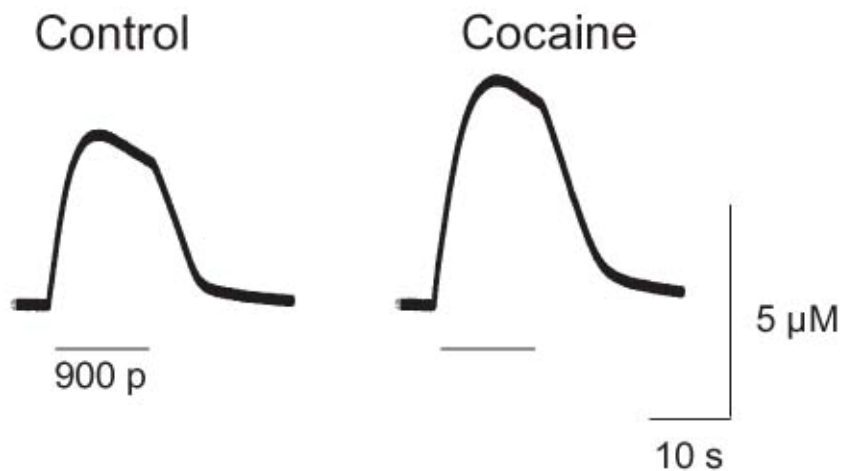
Cocaine and α -methyl-*para*-tyrosine (α MPT) were purchased from Sigma-Aldrich (St. Louis, MO). All drugs were dissolved in saline for intraperitoneal (i.p.) administration.

RESULTS

Effects of cocaine on electrically-evoked dopamine release

Dopamine release was measured in the caudate-putamen of anesthetized mice while the medial forebrain bundle was stimulated with long stimuli (900 pulses, 60 Hz), to probe the multiple compartments of releasable dopamine. At the onset of electrical stimulation in WT mice, dopamine rapidly appeared in the caudate-putamen (**Figure 6.1A**). As the stimulation proceeded, dopamine concentration reached a maximum and then slowly diminished. This biphasic response during stimulation is similar to that previously characterized in rats and attributed to a long-term depression of dopamine release [26]. After the stimulation, dopamine concentration declined rapidly due to neuronal uptake of dopamine [27]. Ten minutes after administration of cocaine (10 mg/kg), the amplitude of the evoked dopamine response ($[DA]_{max}$) increased and reached levels that were 146 ± 26 % of predrug values ($n = 6$ mice). The clearance of dopamine following stimulation appears in

A. WT



B. TKO

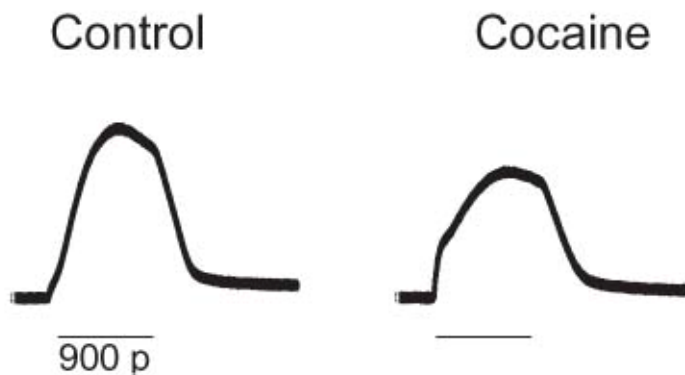


Figure 6.1: Effects of cocaine (10 mg/kg, i.p.) on dopamine release evoked by 900 pulse, 60 Hz electrical stimulations. Predrug traces are displayed on the left and post-injection traces (10-13 minutes following cocaine administration and 40 minutes following the previous stimulation) are shown on the right. **A.** Representative traces from WT mice. **B.** Representative traces from TKO mice. The data are traces from cyclic voltammetric recordings.

Figure 6.1 to be little affected by cocaine. This is because the dopamine concentrations evoked by the long stimuli greatly exceed K_m , the uptake parameter that is affected by cocaine [24]. However, when the rate of uptake is examined at low (submicromolar) dopamine concentrations, near the natural K_m value, changes in K_m following cocaine can be observed. The apparent value of K_m determined under these conditions was $179\% \pm 49\%$ of the predrug value in WT mice ($n = 4$).

This experiment was repeated in synapsin TKO mice to examine the potential role of a reserve pool of dopamine in the response to cocaine. Dopamine responses evoked by the same prolonged stimuli described above had a similar waveform in the TKO mice as in WT mice (**Figure 6.1B**). However, 10 min following cocaine, the amplitude of the stimulated dopamine release was diminished, reaching levels that were only $78 \pm 2\%$ of predrug values ($n = 6$ mice). Thus, the pool mobilized by cocaine appears to be absent in synapsin TKO mice. The apparent value of K_m was $206\% \pm 77\%$ of the predrug value in TKO mice ($n = 6$), a value that is not statistically different from that found in WT mice ($p > 0.05$).

Effects of cocaine on dopamine release following synthesis inhibition

We next examined more directly the ability of cocaine to mobilize the reserve pool of dopamine. This was done by depleting the releasable pool to about 25% of its predrug value [12] by repeatedly applying long-duration stimulus trains (600 pulses at 60 Hz) following administration of α MPT (200 mg/kg, i.p.), a dopamine synthesis inhibitor. Shorter-duration stimuli (24 pulses at 60 Hz) were then applied to probe the effects of cocaine. In the absence

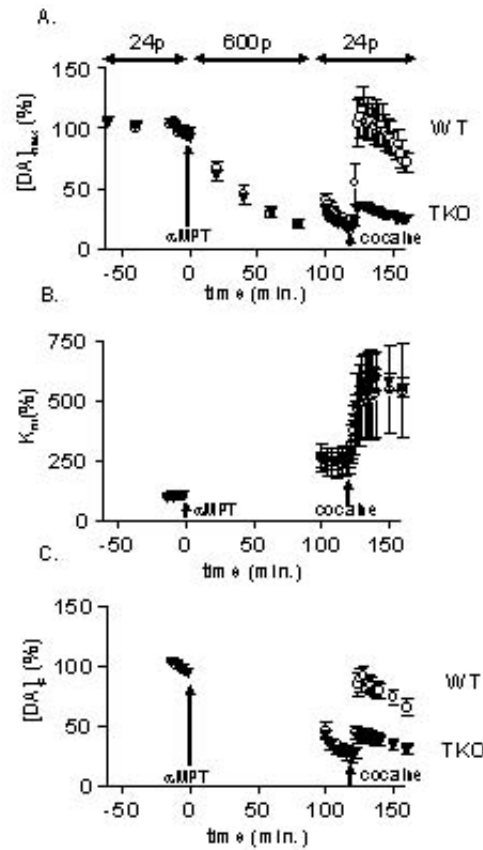


Figure 6.2: Effects of α MPT (200 mg/kg, i.p.) followed by cocaine (10 mg/kg, i.p.) administration on stimulated dopamine release in WT (open circles) and synapsin TKO mice (filled triangles). Dopamine release was electrically evoked by short (24 pulse, 60 Hz, every 2 min) stimulation trains except for the 100 minute interval after α MPT when long (600 pulse, 60 Hz, every 20 min) stimulations were used to deplete dopamine stores, and dopamine was measured by constant potential amperometry. The stimulation pulses (p) in these time domains are indicated at the top of the figure. **A.** The peak neurochemical response ($[DA]_{max}$) to 24- and 600-pulse stimulations as a percentage of the predrug values. **B.** K_m values obtained from modeling of the experimental data expressed as a percentage of the predrug values. **C.** $[DA]_p$ values obtained by neurochemical modeling of the experimental data expressed as a percentage of the predrug value. The data are presented as the mean \pm SEM from measurements in 8 animals for each genotype.

of α MPT, maximal responses to these stimuli were relatively constant over time (**Figure 6.2A**). However, injection of α MPT caused the amount of dopamine released by either type of stimulus to be reduced by approximately 75% (**Figure 6.2A**). Consistent with prior work with other psychostimulants done in rats [12], cocaine (10 mg/kg i.p.) restored the amplitude of responses to electrical stimuli (open symbols in **Figure 6.2A**). Thus, cocaine can enhance dopamine responses, even after the readily releasable pool of dopamine is largely depleted by α MPT. This suggests that cocaine releases dopamine from a pool that is distinct from the readily releasable pool.

To evaluate the role of synapsins in the cocaine-sensitive pool, similar experiments were done in the synapsin TKO mice. As in the WT mice, 600 pulse, 60 Hz stimuli delivered to TKO mice diminished releasable dopamine to about 25% following α MPT (200 mg/kg, i.p.; **Figure 6.2A**). However, subsequent administration of cocaine (10 mg/kg, i.p.) to synapsin TKO mice caused a much smaller increase in the maximal evoked release of dopamine (**Figure 6.2A**). Fitting the responses to 24 pulses with the mathematical model indicated that α MPT caused K_m values to increase slightly in both types of mice; we attribute this to the metabolism of α MPT to p-hydroxyamphetamine [25]. Cocaine administration also caused the same relative change in the K_m for dopamine uptake in both WT and TKO mice (**Figure 6.2B**). In contrast, $[DA]_p$ values, the amount released per stimulus pulse, remained low in TKO mice whereas they returned to near pre- α MPT values in WT mice (**Figure 6.2C**). The $[DA]_p$ values were $42 \pm 4\%$ of initial levels following cocaine in TKO mice and $87 \pm 8\%$ of initial levels in WT mice, values that are statistically different ($p < 0.05$). Thus, the absence of synapsins significantly reduced mobilization of the reserve pool of

dopamine in response to cocaine. These findings indicate that synapsins play a major role in maintaining the dopamine reserve pool and that these proteins serve as a target for cocaine.

DISCUSSION

Cocaine, like many other psychostimulants, is a competitive inhibitor of the DAT [28]. Here we demonstrate that cocaine can also promote dopamine release from the reserve pool. The results are consistent with prior hypotheses that striatal dopamine is segregated into releasable and storage compartments, and that the latter pool can be mobilized by non-amphetamine psychostimulants. The molecular bases of the segregation of these pools of dopamine were revealed through the use of mice lacking synapsin genes. To minimize the possibility of compensation due to redundant functions of synapsin isoforms, we used mice with deletions of all known isoforms of synapsin. In these synapsin TKO mice, both the cocaine-mediated augmentation of release following long stimulus trains and the ability of cocaine to restore release following synthesis inhibition were both dramatically reduced, suggesting that cocaine mobilizes a synapsin-dependent compartment of dopamine vesicles in striatal neurons. These results demonstrate that cocaine increases extracellular dopamine not only by blocking its uptake, but also from mobilizing a synapsin-dependent storage pool.

Cocaine increases dopamine release probability

In addition to inhibiting dopamine uptake, many psychostimulants enhance the amount of releasable dopamine both *in vivo* [9, 12, 29] and *in vitro* [10, 30]. Our work confirms that cocaine also can promote enhanced release probed with long stimuli. DAT

apparently is required for the psychostimulant-induced increase in dopamine release because this increase in dopamine release is not observed in DAT deficient mice [31].

Several lines of evidence point toward the conclusion that cocaine increases dopamine release by mobilizing dopamine from a reserve pool. Early work indicated that dopamine is stored in multiple compartments, with 80% unavailable for immediate release [32, 33]. This normally unavailable dopamine, presumably in a reserve pool, becomes available for release following cocaine as well as other psychostimulants [12]. Our data extend this conclusion by demonstrating that enhanced release following cocaine treatment is most evident when the contribution of the readily releasable pool is minimized: cocaine increased dopamine release by approximately 50% in control conditions (**Figure 6.1A**), but increased release approximately 4-fold after dopamine synthesis was inhibited by α MPT (**Figure 6.2A**). Thus, cocaine preferentially acts upon a pool of dopamine that is not readily releasable and does not depend upon continuous synthesis of dopamine.

Synapsins regulate releasable stores in dopamine neurons

Although early investigators of catecholamine metabolism described a reserve compartment for the intracellular storage of dopamine [32, 34], its nature and subcellular location have largely remained unclear. In nerve terminals using other transmitters, such as glutamate and GABA, a subset of vesicles is sequestered to the cytoskeleton by synapsins [19, 21]. In synapsin TKO mice, we found that dopamine release could still be evoked electrically, but cocaine was much less able to enhance electrically evoked dopamine release than in WT animals. This demonstrates that synapsins also are important for the cocaine-sensitive storage pool in dopaminergic terminals. In fact, dopamine release evoked by long

stimuli was actually diminished by cocaine in synapsin TKO mice. This presumably is due to the absence of a reserve pool in combination with the action of cocaine on dopamine uptake, which would be expected to impair recycling of dopamine into the releasable pool and cause a net decrease in dopamine release.

These findings indicate that cocaine can increase dopamine release by mobilizing synapsin-bound vesicles that comprise the dopamine storage pool. How cocaine interacts with synapsin is unclear. Cocaine is known to increase dopamine release from striatal terminals even when isolated from their cell bodies [10], meaning that cocaine must act locally within the presynaptic terminal. In some cells, cocaine can enhance presynaptic Ca^{2+} influx [35, 36] and chronic administration of cocaine increases the sensitivity of released dopamine to Ca^{2+} channel blockers [37]. It is thought that Ca^{2+} -dependent phosphorylation of synapsins is required for mobilization of vesicles from the reserve pool during electrical stimulation [19]. Thus, it is possible that cocaine and other psychostimulants enhance dopamine release by increasing presynaptic Ca^{2+} influx and thereby mobilizing synaptic vesicles as a result of Ca^{2+} -dependent phosphorylation of synapsins.

Implications of synapsin regulation of dopamine release

Dopamine neurons are phasically activated by incentive cues. Dopamine release then modulates neuronal signals passing through medium spiny neurons in striatum by gating glutamatergic afferents [38] and promotes selection of an appropriate motor response. By interacting with synapsins, cocaine can switch dopamine neurons into a mode of sustained dopamine release that would be expected to elevate sensory cue reactivity. Indeed, amplification of sensorimotor integration by cocaine is consistent with the effects of this drug

on mobilization of dopamine from the storage pool because neither effect is prevented by inhibiting dopamine synthesis [5]. Overall, the synapsin-mediated effect of cocaine on the dopamine reserve pool, in combination with other forms of plasticity in the mesolimbic system [39-42], may contribute considerably to the highly addictive nature of psychostimulants.

REFERENCES

1. Schultz, W., *Predictive reward signal of dopamine neurons*. (vol 80, pg 1, 1998). Journal of Neurophysiology, 1998. **80**(6): p. U32-U32.
2. Taghzouti, K., et al., *Behavioral-Study after Local Injection of 6-Hydroxydopamine into the Nucleus Accumbens in the Rat*. Brain Research, 1985. **344**(1): p. 9-20.
3. Roitman, M.F., et al., *Dopamine operates as a subsecond modulator of food seeking*. Journal of Neuroscience, 2004. **24**(6): p. 1265-1271.
4. Phillips, P.E.M., et al., *Subsecond dopamine release promotes cocaine seeking* (vol 422, pg 614, 2003). Nature, 2003. **423**(6938): p. 461-461.
5. Davis, M., *Cocaine - Excitatory Effects on Sensorimotor Reactivity Measured with Acoustic Startle*. Psychopharmacology, 1985. **86**(1-2): p. 31-36.
6. Childress, A.R., et al., *Limbic activation during cue-induced craving for cocaine and for natural rewards*. Biological Psychiatry, 1999. **45**(8S): p. 53s-53s.
7. Bauman, P. and L. Maitre, *Is drug inhibition of dopamine uptake a misinterpretation of in vitro experiments?* Nature, 1976. **264**: p. 789-790.
8. Jones, S.R., P.A. Garris, and R.M. Wightman, *Different Effects of Cocaine and Nomifensine on Dopamine Uptake in the Caudate-Putamen and Nucleus-Accumbens*. Journal of Pharmacology and Experimental Therapeutics, 1995. **274**(1): p. 396-403.
9. Stamford, J., Z. Kruk, and J. Millar, *Dissociation of the actions of uptake blockers upon dopamine overflow and uptake in the rat nucleus accumbens: in vivo voltammetric data*. Neuropharmacology, 1989. **28**: p. 1383-1388.
10. Lee, T.H., et al., *Differential time-course profiles of dopamine release and uptake changes induced by three dopamine uptake inhibitors*. Synapse, 2001. **41**(4): p. 301-310.
11. Shore, P.A., *Actions of Amfonelic Acid and Other Non-Amphetamine Stimulants on Dopamine Neuron*. Journal of Pharmacy and Pharmacology, 1976. **28**(11): p. 855-857.
12. Ewing, A.G., J.C. Bigelow, and R.M. Wightman, *Direct in vivo monitoring of dopamine released from two striatal compartments in the rat*. Science, 1983. **221**(4606): p. 169-71.
13. Neher, E., *Vesicle pools and Ca²⁺ microdomains: New tools for understanding their roles in neurotransmitter release*. Neuron, 1998. **20**(3): p. 389-399.

14. Pieribone, V.A., et al., *Distinct Pools of Synaptic Vesicles in Neurotransmitter Release*. Nature, 1995. **375**(6531): p. 493-497.
15. Rosenmund, C. and C.F. Stevens, *Definition of the readily releasable pool of vesicles at hippocampal synapses*. Neuron, 1996. **16**(6): p. 1197-1207.
16. Kuromi, H. and Y. Kidokoro, *Two distinct pools of synaptic vesicles in single presynaptic boutons in a temperature-sensitive Drosophila mutant, shibire*. Neuron, 1998. **20**(5): p. 917-925.
17. Duncan, R.R., et al., *Functional and spatial segregation of secretory vesicle pools according to vesicle age*. Nature, 2003. **422**(6928): p. 176-180.
18. Richards, D.A., et al., *Synaptic vesicle pools at the frog neuromuscular junction*. Neuron, 2003. **39**(3): p. 529-541.
19. Greengard, P., et al., *Synaptic Vesicle Phosphoproteins and Regulation of Synaptic Function*. Science, 1993. **259**(5096): p. 780-785.
20. Hilfiker, S., et al., *Synapsins as regulators of neurotransmitter release*. Philosophical Transactions of the Royal Society of London Series B-Biological Sciences, 1999. **354**(1381): p. 269-279.
21. Gitler, D., et al., *Different presynaptic roles of Synapsins at excitatory and inhibitory synapses*. Journal of Neuroscience, 2004. **24**(50): p. 11368-11380.
22. Gitler, D., et al., *Molecular determinants of synapsin targeting to presynaptic terminals*. Journal of Neuroscience, 2004. **24**(14): p. 3711-3720.
23. Venton, B.J., K.P. Troyer, and R.M. Wightman, *Response times of carbon fiber microelectrodes to dynamic changes in catecholamine concentration*. Analytical Chemistry, 2002. **74**(3): p. 539-546.
24. Venton, B.J., et al., *Real-time decoding of dopamine concentration changes in the caudate-putamen during tonic and phasic firing*. Journal of Neurochemistry, 2003. **87**(5): p. 1284-1295.
25. Joseph, J.D., et al., *Dopamine autoreceptor regulation of release and uptake in mouse brain slices in the absence of D-3 receptors*. Neuroscience, 2002. **112**(1): p. 39-49.
26. Montague, P.R., et al., *Dynamic gain control of dopamine delivery in freely moving animals*. Journal of Neuroscience, 2004. **24**(7): p. 1754-1759.
27. Garris, P.A., et al., *Efflux of Dopamine from the Synaptic Cleft in the Nucleus-Accumbens of the Rat-Brain*. Journal of Neuroscience, 1994. **14**(10): p. 6084-6093.

28. Wu, Q., et al., *Preferential increases in nucleus accumbens dopamine after systemic cocaine administration are caused by unique characteristics of dopamine neurotransmission*. Journal of Neuroscience, 2001. **21**(16): p. 6338-6347.
29. Stamford, J.A., Z.L. Kruk, and J. Millar, *Measurement of stimulated dopamine release in the rat by in vivo voltammetry: the influence of stimulus duration on drug responses*. Neurosci Lett, 1986. **69**(1): p. 70-3.
30. Hafizi, S., P. Palij, and J.A. Stamford, *Activity of two primary human metabolites of nomifensine on stimulated efflux and uptake of dopamine in the striatum: in vitro voltammetric data in slices of rat brain*. Neuropharmacology, 1992. **31**(8): p. 817-24.
31. Jones, S.R., et al., *Profound neuronal plasticity in response to inactivation of the dopamine transporter*. Proceedings of the National Academy of Sciences of the United States of America, 1998. **95**(7): p. 4029-4034.
32. Javoy, F. and J. Glowinski, *Dynamic characteristic of the 'functional compartment' of dopamine in dopaminergic terminals of the rat striatum*. Journal of Neurochemistry, 1971. **18**: p. 1305-1311.
33. Korf, J., L. Grasdijk, and B.H.C. Westerink, *Effects of Electrical-Stimulation of Nigrostriatal Pathway of Rat on Dopamine Metabolism*. Journal of Neurochemistry, 1976. **26**(3): p. 579-&.
34. Doteuchi, M., C. Wang, and E. Costa, *Compartmentation of Dopamine in Rat Striatum*. Molecular Pharmacology, 1974. **10**(2): p. 225-234.
35. Premkumar, L.S., *Selective potentiation of L-type calcium channel currents by cocaine in cardiac myocytes*. Molecular Pharmacology, 1999. **56**(6): p. 1138-1142.
36. Yermolaieva, O., et al., *Cocaine- and amphetamine-regulated transcript peptide modulation of voltage-gated Ca²⁺ signaling in hippocampal neurons*. Journal of Neuroscience, 2001. **21**(19): p. 7474-7480.
37. Pierce, R.C. and P.W. Kalivas, *Repeated cocaine modifies the mechanism by which amphetamine releases dopamine*. Journal of Neuroscience, 1997. **17**(9): p. 3254-3261.
38. Floresco, S.B., et al., *Modulation of hippocampal and amygdalar-evoked activity of nucleus accumbens neurons by dopamine: Cellular mechanisms of input selection*. Journal of Neuroscience, 2001. **21**(8): p. 2851-2860.
39. Wolf, M.E., *The role of excitatory amino acids in behavioral sensitization to psychomotor stimulants*. Progress in Neurobiology, 1998. **54**(6): p. 679-720.

40. Robinson, T.E. and B. Kolb, *Alterations in the morphology of dendrites and dendritic spines in the nucleus accumbens and prefrontal cortex following repeated treatment with amphetamine or cocaine*. European Journal of Neuroscience, 1999. **11**(5): p. 1598-1604.
41. Ungless, M.A., et al., *Single cocaine exposure in vivo induces long-term potentiation in dopamine neurons*. Nature, 2001. **411**(6837): p. 583-587.
42. Liu, Q.S., L. Pu, and M.M. Poo, *Repeated cocaine exposure in vivo facilitates LTP induction in midbrain dopamine neurons*. Nature, 2005. **437**(7061): p. 1027-1031.